

Research article

Biodegradation of various grades of polyethylene microplastics by *Tenebrio molitor* and *Tenebrio obscurus* larvae: Effects on their physiology



Meng-Qi Ding^a, Jie Ding^{a,*}, Zhi-Rong Zhang^b, Mei-Xi Li^a, Chen-Hao Cui^a, Ji-Wei Pang^c, De-Feng Xing^a, Nan-Qi Ren^a, Wei-Min Wu^d, Shan-Shan Yang^{a,*}

^a State Key Laboratory of Urban Water Resource and Environment, School of Environment, Harbin Institute of Technology, Harbin, 150090, China

^b College of Wildlife and Protected Area, Northeast Forestry University, Harbin, 150040, China

^c China Energy Conservation and Environmental Protection Group, CECEP Digital Technology Co., Ltd, Beijing, 100089, China

^d Department of Civil and Environmental Engineering, William & Cloy Codiga Resource Recovery Center, Stanford University, Stanford, CA, 94305, USA

ARTICLE INFO

Keywords:

Mealworms

Polyethylene physical-chemical properties

Microbiome

Metabolism

Physiology responses

Ecotoxicity

ABSTRACT

Polyethylene (PE) is the most productive plastic product and includes three major polymers including high-density polyethylene (HDPE), linear low-density polyethylene (LLDPE) and low-density polyethylene (LDPE) variation in the PE depends on the branching of the polymer chain and its crystallinity. *Tenebrio obscurus* and *Tenebrio molitor* larvae biodegrade PE. We subsequently tested larval physiology, gut microbiome, oxidative stress, and PE degradation capability and degradation products under high-purity HDPE, LLDPE, and LDPE powders (<300 µm) diets for 21 days at 65 ± 5% humidity and 25 ± 0.5 °C. Our results demonstrated the specific PE consumption rates by *T. molitor* was 8.04–8.73 mg PE • 100 larvae⁻¹·day⁻¹ and by *T. obscurus* was 7.68–9.31 for LDPE, LLDPE and HDPE, respectively. The larvae digested nearly 40% of the ingested three PE and showed similar survival rates and weight changes but their fat content decreased by 30–50% over 21-day period. All the PE-fed groups exhibited adverse effects, such as increased benzoquinone concentrations, intestinal tissue damage and elevated oxidative stress indicators, compared with bran-fed control. In the current study, the digestive tract or gut microbiome exhibited a high level of adaptability to PE exposure, altering the width of the gut microbial ecological niche and community diversity, revealing notable correlations between *Tenebrio* species and the physical and chemical properties (PCPs) of PE-MPs, with the gut microbiome and molecular weight change due to biodegradation. An ecotoxicological simulation by T.E.S.T. confirmed that PE degradation products were little ecotoxic to *Daphnia magna* and *Rattus norvegicus* providing important novel insights for future investigations into the environmentally-friendly approach of insect-mediated biodegradation of persistent plastics.

1. Introduction

Polyethylene (PE) is a synthetic polymer derived from petroleum and is widely used in the production of plastics, accounting for 26.3% of global production of 400.3 million tonnes (PlasticsEurope, 2024). The accumulation and pollution of waste PE products has become a significant environmental or public health problem, attracting widespread attention in the fields of solid waste management and environmental toxicology (Ding et al., 2023; Shi et al., 2022; Zhang et al., 2022a). Low-density polyethylene (LDPE), linear low-density polyethylene (LLDPE) and high-density polyethylene (HDPE), and are the major

products of PE (Wilkes and Aristilde, 2017). HDPE has long linear chains with minimal or no branching and a high degree of crystallinity (60–80%). LLDPE has a medium crystallinity range of 20–60% (Kong et al., 2003). It is composed of linear molecules with more short chain branching than HDPE (Ojeda et al., 2011a). Its crystallinity is low, ranging from 40 to 50% (Yu et al., 2014). LDPE, on the other hand, has a high quantity of long chain branching, with an average branch length of several hundred carbon atoms, as well as small chain branching that is 2–6 carbon atoms long. According to Yang et al. (2022), the physical properties of different polymers make them suitable for various applications and also affect their degradability in different environments, i.e.,

* Corresponding author.

** Corresponding author.

E-mail addresses: dingjie123@hit.edu.cn (J. Ding), shanshanyang@hit.edu.cn (S.-S. Yang).

LDPE degrades faster than LLDPE and HDPE.

Disposal of plastics, including landfilling, mechanical recycling, and incineration, has several drawbacks and limitations for plastic waste management. Since 1970s, the biodegradation of PE products, particularly LDPE, has been investigated using microorganisms from diverse environmental sources, including sludge, soil, landfill, seawater and compost (Ghatge et al., 2020; Restrepo-Florez et al., 2014; Ru et al., 2020). The results of study indicate that PE is resistant to biodegradation, with a half-life that can range from weeks to months or even years (Shah et al., 2008). Biodegradation of PE in natural environments is believed to occur only after thermal or photo-oxidation (Lambert and Wagner, 2017; Shah et al., 2008). Previous studies using microbial cultures and enzymes have also shown that the biodegradability of PE polymers is influenced by the physical properties (PCPs) of the polymers, such as molecular weight, long and short-chain branching, C-atom number of polymer chains, hydrophobicity, and crystallinity, etc. (Ojeda et al., 2011b; Wilkes and Aristilde, 2017; Yang et al., 2022a). A study by Chiellini et al. (2003) demonstrated a 50% reduction in mass of PE materials with a molecular weight of less than 1.5 kDa over a period of 120 days due to microbial degradation. However, for higher molecular weight PE, it took more than two months for a PE-degrading *Enterobacter asburiae* YT1 and *Bacillus* sp. YP1 to degrade about 6.5% and 11.3% of commercial LDPE film with a molecular weight of 88.2 and Mn of 27.7 kDa (Yang et al., 2014). "Biodegradation" is a term that refers to the degradation of a substance by enzymes present in living organisms, primarily through microbial activities. This process involves the decomposition of organic matter, as described in Wikipedia. Biodegradation of persistent plastics is an attractive solution due to its cost effectiveness and environmental friendliness (Sanchez-Hernandez, 2021). This process can be carried out either on-site or through natural mechanisms, making it the most favourable method for environmental remediation. Although "biodegradation" is traditionally associated with microbial degradation, it has also been employed to refer to degradation facilitated by insects.

To date, since 2015, *T. molitor* fed PS styrofoam with number average molecular weights (Mn) of 40,430 and weight average molecular weights (Mw) of 124,200 as a sole diet by Yang et al. (2015a), 47.7% of the ingested styrofoam carbon was converted into CO₂ within 16 days, researchers have been attracted to using insects to degrade plastic polymers. Reports of insect biodegradation of plastics have focused primarily on the larvae of *Tenebrio*, *Molitor*, *T. obscurus*, and *Zophobas atratus* (Tenebrionidae) (Robinson, 2005), and *Galleria mellonella* (Pyralidae), probably and partially, due to their high commercial availability, and chew, ingest and biodegrade plastic at rates on an hourly basis. Biodegradation of LDPE and PS were the main plastics targeted by Tenebrionidae in these studies (Brandon et al., 2018; Peng et al., 2019; Yang et al., 2015a, 2015b, 2021a, 2021c). They also biodegrade PVC, PP and PUR (Luo et al., 2021; Peng et al., 2020; Yang et al., 2021b). Additionally, the insects belonging to Lepidoptera, Pyralidae moths also showed biodegradation of PE, including *G. mellonella* (Bombelli et al., 2017; Kong et al., 2019; Yang et al., 2014), Indian meal moth *Plodia interpunctella* (Yang et al., 2014), *Achroia grisella* (Kundungal et al., 2019) and *Spodoptera frugiperda* (Zhang et al., 2022b).

Both *T. molitor* and *T. obscurus* larvae are not only two widely investigated plastic-degrading insect larvae (Wu and Criddle, 2021; Yang et al., 2023b), but also are commercially reared for animal feed and insect protein, typically being fed with wheat bran (WB) (Ding et al., 2023; Peng et al., 2019; Yang et al., 2021c). Our previous work has shown that both species can rapidly biodegrade LDPE, LLDPE and HDPE (Yang et al., 2021c, 2022). Studies of LDPE biodegradation by these two species have demonstrated that under nutrient-poor conditions, coordination of gut microbiome carbon and nitrogen metabolism is necessary for energy and nutrition acquisition during plastic degradation (Ding et al., 2023; Yang et al., 2023a). Although *T. molitor* and *T. obscurus* have distinct behaviours (Peng et al., 2019; Robinson, 2005), both species can adapt to LDPE diets by altering their gut microbiota or

microbiome structure (Dai et al., 2022; Welti et al., 2020) to ensure their capacity to survive using PE as their sole source of both energy and carbon within a 3–5 week period (Lou et al., 2020, 2021; Przemieniecki et al., 2020; Woo et al., 2020; Yang et al., 2021a, 2021b, 2021c, 2022). Previous research on reported that a decrease in gut microbial community similarity occurs after larvae switch to a plastic-based diet, such as LDPE, PS, and etc. (Brandon et al., 2018; Peng et al., 2019, 2021; Przemieniecki et al., 2020; Ruiz Barrionuevo et al., 2022a, 2022b; Yang et al., 2022, Yang et al., 2023a). However, the majority of reports on microbiomes associated with PE degradation by insect larvae have focused on LDPE (Brandon et al., 2018; Peng et al., 2019; Yang et al., 2021c).

During plastics biodegradation, *Tenebrio* larvae are directly exposed to PE microplastics (MPs), through biofragmentation of ingested plastic foams or particles into fragments by chewing, grinding, and digestion in the gut. Studies on other macroinvertebrates have shown that long-term exposure to MPs can cause biological toxicity, causing mechanical damage and the onset of inflammatory responses in *Corbicula fluminea*, mice and zebrafish (Li et al., 2021). The gut is a vital line of defence against exogenous substances, as well as being an essential organ for immunity, digestion and absorption in insects. When the gut microbiota becomes imbalanced or are mechanically stimulated, various inflammatory and immune cells are activated, leading to intestinal inflammation (Baeckhed et al., 2005; Li et al., 2021; Suzuki et al., 2004). However, the extent to which gut health reflects the effects of PE-MPs with different PCPs on *Tenebrio* larvae during plastic degradation, has not been clearly elucidated. Our previous studies found that different metabolic intermediates were generated when *T. molitor* and *T. obscurus* larvae ingested and digested HDPE, LLDPE and LDPE. The degradation intermediates formed may also affect on *T. obscurus* and *T. molitor* larvae.

For more than a decade, PE has been the top plastic in the world, and it is a promising sustainable technology and green strategy to utilize the mealworms, which are macroinvertebrates with the ability to degrade plastics, in the biodegradation of PE. To the best of our knowledge, no studies have comprehensively addressed the comparison of the impacts of PE type (LDPE, LLDPE and HDPE) on larval physiology, gut microbiome and oxidative stress (at a physiological or biochemical level). In addition, in the long run, the larvae degrade microplastics and then excrete plastic into the ecosystem, and it is important to investigate whether their frass contain toxic substances that are harmful to aquatic and terrestrial organisms in the environment and even to human health. The environmental toxicology of microplastics produced by plastic biofragmentation has become an emerging environmental issue (Peng et al., 2023b; Shi et al., 2022). This study was performed by investigating the physiology of the larvae including survival, growth and biomass (fat, crude protein, carbohydrate and benzoquinone) composition status of *T. molitor* and *T. obscurus* larvae fed with different PE polymers viz., LDPE, HDPE and LLDPE versus those fed a conventional diet of wheat bran (WB) diet; microbiome by assessing changes in their gut microbiomes through 16S rRNA gene sequencing; and access to gut damage by observing larval histopathology. Bioindicators including the total antioxidant capacity (T-AOC), superoxide dismutase (SOD) and malondialdehyde (MDA) were selected to evaluate the oxidative stress response to MP exposure in *T. molitor* and *T. obscurus* larvae in relation to the three PE types. It has been reported that when mealworms are exposed to microplastic contaminants, the organism's resistance to environmental stress is increased due to elevated levels of these indicators (Peng et al., 2023b). In addition, quantitative structure-activity relationship (QSAR) prediction was performed using Toxicity Estimation Software Tool (T.E.S.T; US EPA), to value the toxicity of degradation products.

2. Materials and methods

2.1. Sources of *Tenebrio* larvae

T. molitor larvae were procured from the Dafa Birds and Flower Market in Harbin, China while *T. obscurus* larvae were procured from a Breeding Farm in Zaozhuang, Shandong, China. The dealers claimed that the larvae were fed a diet without antibiotics.

2.2. PE materials

The high-purity PE powders (size: <300 µm) of LDPE, HDPE, and LLDPE were purchased from Shanghai Plastics Trading Co., Ltd., Shanghai, China. The molecular weights are Mn 42.2, 93.2, and 59.5 kDa; Mw 110.5, 222.5, and 182 kDa; and size averaged molecular weight (Mz) 216.1, 456.5, and 408.8 kDa for LDPE, LLDPE, and HDPE, respectively (Table S1). No catalysts or additives were present according to manufacture (Table S2). Wheat bran (WB) was purchase from agricultural market in Harbin, China. All analytical grade chemicals used for analyses were analytical grade from Sinopharm Chemical Reagent Co., Ltd., Beijing, China, were all utilized in the studies. Beijing Aoboxing Bio-Tech Co., Ltd provided the agar.

2.3. Biodegradation tests

Biodegradation of HDPE, LLDPE and LDPE by *T. obscurus* and *T. molitor* larvae were performed. To allow the larvae to naturally and effectively ingest and biodegrade the MP particles, the respective PE powders were mixed with agar (0.9:25, w/w) as an adhesive. This method has been previously used and reported in studies by Cappellozza et al. (2019); Peng et al. (2021); Yang et al. (2022). The larvae of *T. molitor* and *T. obscurus* were fed with high-purity HDPE, LLDPE, and LDPE powders (25 g) mixed with agar (DI Water 30 ml, 3%, w/w) compared to agar with WB as the control diet. Prior to starting the experimental diets, all tested larvae were starved for 48 h to empty their guts. Initially, 7g of food was provided to *T. obscurus* and *T. molitor* larvae in 1000 ml food-grade rigid polypropylene incubators. Food freedom was ensured during the experiment, and each incubator contained 400 larvae. The experiments were conducted in triplicate. The larvae fed with WB served as the control group. To prevent cannibalism, dead mealworms were immediately removed. (Ding et al., 2023; Peng et al., 2019). All larval incubators were kept in an artificial climate chamber (250L in volume) (Artificial climate incubator, Shanghai Shuli, Shanghai, China) for 21 days at 65 ± 5% humidity and 25 ± 0.5 °C.

Every seven days throughout the experimental period, the number of live and dead larvae in each group was counted to determine the larval survival rates (SRs) (Peng et al., 2021; Wu and Criddle, 2021; Yang et al., 2021c). The average weight of larvae was determined. Both species were fed WB for two weeks, although corn flour is the preferred food of *T. obscurus* (Ding et al., 2023; Peng et al., 2019b). A detailed description of the diet fed to *Tenebrio* larvae is available in the supporting information (SI M1 and Table S3).

2.4. Measurement of PE particles

PE-MPs present in the *Tenebrio* larvae frass were extracted using a Fenton system (Qin et al., 2015) combined with an olive oil-based extraction method (Scopetani et al., 2020) developed based on previous reports after the frass material was ground using a pestle and dried (Yang et al., 2021c). More details is available in the supporting information (SI M2 and Figs. S1–2).

2.5. Analytical methods

The molecular weight values (Mw, Mn, and Mz) of the virgin and residual PE-MPs were ascertained by high-temperature gel permeation

chromatography (HT-GPC) (PL-GPC 220, Agilent Technologies, Inc., USA) analysis, respectively. It should be noted that the reduction in molecular weight (%) is shown as a positive value; thus, an increase in molecular weight corresponds to a negative value.

Using a Nicolet iS50 FTIR Spectrometer (Thermo Fisher Scientific, U.S.A.), Fourier transform infrared (FTIR) spectroscopy was utilized to identify the primary functional groups of virgin PE-MPs compared to frass residues following transit through the digestive system. Furthermore, the PE-MPs' oxidation was evaluated using the Carbonyl index (CI), which was computed in accordance with Lessa Belone et al. (2021); Prata et al. (2019). For LDPE, LLDPE, and HDPE, the intensity of the carbonyl peak (C=O) in the range of 1715–1735 cm⁻¹ was divided by the intensity of 1471 cm⁻¹ (as a reference peak).

Using a Bruker Avance 600 MHz NMR spectrometer (Bruker Corporation, Germany) for proton nuclear magnetic resonance and an Agilent GC/MS instrument (7890B-5977 B GC/MS from Agilent Technologies, USA) in conjunction with a PY-3030D pyrolyzer unit (EGA/PY-3030D, Frontier, Japan) from Frontier Laboratories for Pyrolysis-gas chromatography/mass spectrometry (Py-GC/MS). All analytical procedures are described in detail in the supporting information (SI M2) and were performed according to established methods for characterizing plastic biodegradation, as documented in previous publications (Brandon et al., 2018; Wu and Criddle, 2021; Yang et al., 2022). Each analysis was performed in triplicate to ensure reliability.

2.6. Determination of biomass composition

At the end of the test period (day 21), 50 larvae from each test group were euthanized by low temperature (-80 °C) lyophilization (LGJ-12F, Foring Science Instrument Technology Development Co. Ltd., Beijing, China), then crushed and mixed under liquid nitrogen conditions. Subsequently, the larval biomass was collected for use in the determination of biomass nutrient concentration levels. The total concentrations of carbohydrates (food safety testing standard GB/T 15,672-2009), crude fats (GB 5009.6–2016), crude proteins (GB/T 6433-2006) and benzoquinones were determined in triplicate in order to determine the physiological indexes for larvae. GC-MS analysis was performed to determine the fatty acid content (GB 5009.168–2016) of every exposure group. The Cys content was determined using a Cys assay kit (YX-W-A905) from Sinobestbio Co. Ltd. (Shanghai, China). A microplate reader (FlexA-200, ALLSHENG, Hangzhou, China) (600 nm absorbance) was used to measure the concentration. A detailed description of the analytical methods used is provided in the SI (M1) (Peng et al., 2019, 2022; Zielińska et al., 2021).

2.7. 16S rRNA gene sequencing

The gut tissues and its contents of 20 randomly selected larvae were collected from each group at the end of the 21 day test period for microbial community analysis. Samples were rinsed twice with 8.5% NaCl after decontamination by immersion in 75% ethanol for 1–2 min to obtain the gut tissue. Before being used, all samples were preserved in sterile freeze-storage tube and kept at -80 °C. Whole samples were sent to Shanghai Majorbio Bio-Pharm Technology Co. Ltd. (Shanghai, China) for microbial community analysis, with a detailed description of the DNA extraction and PCR amplification methods used provided in the SI (M2). Operational Taxonomic Units (OTUs) were identified from the sequencing results by clustering sequences with an identity threshold of 0.97 using UPARSE (v. 11). Chimeric sequences were identified and deleted using FLASH (v. 1.2.11). The Silva 138 16S rRNA database was used to analyse the taxonomy of each 16S rRNA gene sequence by the Ribosomal Database Project (RDP) classifier (v. 2.13), against a 70% confidence threshold. For each microbiome, niche width analysis, non-metric multidimensional scaling (NMDS; based on Abund-Jaccard distance), permutational multivariate analysis of variance (PERMANOVA; using the 999 permutations of the Adonis function), differential

abundance and indicator analysis were conducted by calculating the compositional similarities of the gut microbiomes for all 32 samples, with results plotted using the online Majorbio Cloud Platform and R v. 4.2.3. Furthermore, null model analysis was carried out to classify community pairings into groups (SI M3) (Jiao et al., 2020; Stegen et al., 2013) and assess the variation in both phylogenetic and taxonomic diversity (Dini-Andreote et al., 2015; Jiao et al., 2020; Stegen et al., 2013; Tripathi et al., 2018).

2.8. Sensitivity analysis of test variables

Relative generic abundance, diet and host-specificity metadata (e.g., larvae source or species) and PE-MP PCPs were used for the Abund Jaccard distance-based redundancy analysis (dbRDA) using R package (v. 3.3.1). Variation partitioning analysis (VPA) (R vegan package) was used to determine the explanatory value (%) for significant response variables, such as larval diet and larval species.

Partial least squares structural equation modeling (PLS-SEM) was performed using SmartPLS3 software with the following variables: *Tenebrio* species (*T. molitor* versus *T. obscurus*), microbiome (based on diet related genus abundances and host-specificity), and the PCPs of PE-MPs (WCAs, PE type, Mn, Mw, Mz and crystallinity degree). The relationship between variables was defined by the path coefficients. The statistical goodness of fit (GOF) was used to select the target model from all the created models, based on the models overall predictive power (Liao et al., 2018; Wagg et al., 2014; Zhou et al., 2020).

2.9. Hub KO analysis

The analysis of differentially expressed genes based on weighted gene co-expression network analysis (WGCNA) have been powerful, effective, and widely used methods to explore relationships between genes (Núria et al., 2022; Wu et al., 2020). These methods have successfully uncovered characteristic genes in key pathways and identified functional gene clusters with co-regulated profiles. This allows for the construction of an accurate network of hub genes and environmental traits by focusing on gene expression datasets and microarray analysis. Kyoto Encyclopedia of Genes and Genomes (KEGG) and WGCNA (SI M3) analyses were combined to screen for hub KEGG Orthology (KO) enrichment (based on the Tax4Fun2 program on the online Majorbio Cloud Platform and R v. 4.2.3) corresponding to metabolism (Ren et al., 2022; Wu et al., 2021).

2.10. In vivo oxidative stress and in vitro cytotoxicity simulation assays

To establish whether oxidative stress and damage could be induced by PE MPs in *Tenebrio* larvae, which have been shown previously to have a high capacity for plastic biodegradation, the levels of T-AOC, SOD and MDA were determined in larvae at the end of the test period (day 21). All experimental procedures followed the manufacturer's instructions (SI M4). In addition, single larva was randomly selected from each group and fixed in 4% (v/v) formaldehyde, embedded in paraffin, then sectioned (4 μ m thickness) and finally stained with hematoxylin and eosin (H&E) prior to microscopic examination. Finally, degradation intermediates/compounds of three types of PE were evaluated through QSAR prediction using T.E.S.T. to estimate their acute oral toxicity (LD50) in *Rattus norvegicus* and *Daphnia magna* (48 h LC50) as well as their potential for developmental toxicity.

2.11. Statistical analysis

ANOVA analysis was carried out to assess the differences in SRs, AWCRs and microbial diversity. To evaluate variations due to diet and species, the Student's t-test was conducted with Tukey's correction. All reported p-values were adjusted and error values were expressed as the average value \pm standard deviation. Statistical analysis was conducted

using Origin (v. 2022b).

3. Results and discussion

3.1. Biodegradation of PE-MPs in *T. molitor* and *T. obscurus* larvae

Both *T. molitor* and *T. obscurus* larvae consumed all three types of PE polymers. At the end of the test, the SPECR by *T. molitor* were 8.26 ± 0.28 , 8.73 ± 0.19 , and 8.04 ± 0.06 mg PE \bullet 100 larvae $^{-1}$.day $^{-1}$ for LDPE, LLDPE and HDPE, respectively. The residual PE polymer contents in the frass on day 21 were $52.23 \pm 7.22\%$, $59.17 \pm 12.16\%$, and $68.72 \pm 8.96\%$ for LDPE, LLDPE and HDPE, respectively. The SPECR of *T. obscurus* larvae were 9.31 ± 0.35 , 8.03 ± 0.08 , and 7.68 ± 0.13 mg PE \bullet 100 larvae $^{-1}$.day $^{-1}$ for LDPE, LLDPE and HDPE, respectively, with respective residual PE contents in the frass of $51.82 \pm 8.45\%$, $62.00 \pm 5.25\%$, and $64.52 \pm 14.65\%$ (Table 1). The results indicated that the larvae of both species showed biodegradability as LDPE > LLDPE > HDPE.

The numbers of *T. molitor* and *T. obscurus* larvae fed with PE polymers in all groups decreased over test period. The SRs of both *T. molitor* fed with PE were lower than those of Controls fed with bran with an order of WB > LDPE > HDPE > LLDPE (Fig. 1A and Table 1). The SRs of *T. obscurus* larvae in each group were not significantly different, and WB diet group was slightly lower than that of the PE diet group, suggesting that the PE plastic diet did not cause a decrease in the SRs of the larvae. No intact dead larvae were observed during the experiment. The larvae of the *Tenebrio* genus (e.g., *T. molitor*, *T. obscurus* and *Z. atratus*) have the innate behavior of cannibalism (Ding et al., 2023; Yang et al., 2021b, 2021c), and the reduced SR of the larvae in the present study was mainly caused by cannibalism of the larvae. In addition, at the end of the 21-day test, the larvae fed with WB had significantly higher AWCRs than those fed with PE polymers in both species of larvae ($P < 0.01$). This was expected due to the nutrition-rich WB diets enhancing the larval average weight (Fig. 1B and Table 1 and S3).

3.2. Verification of biodegradation

The biodegradation/depolymerization of the three PE polymers was verified by changing in PE structures and oxidization of residual polymers. Molecular weight changes were observed as LDPE from the frass of *T. obscurus* and *T. molitor* larvae with decreasing of Mn from 93.2 to 67.6 versus 69, Mw from 222.5 to 158.9 versus 162.4, and Mz from 456.5 to 306.5 versus 315 kDa; while LLDPE with increasing of Mn from 42.2 to 71.6 versus 82.2, Mw from 110.5 to 179.2 versus 193.5, and Mz from 216.1 to 361.1 versus 379.1 kDa. In addition, the residual HDPE's molecular weight (Mn and Mw) was increased, i.e., Mn from 59.5 to 77.4 versus 80.8, Mw from 180.2 to 200.2 and 201.6 kDa, but Mz was remained almost unchanged (it reduced from 408.8 to 404.6 kDa and increased from 408.8 to 415.5 kDa, respectively). The three PE polymers biodegraded similarly in *T. obscurus* and *T. molitor* larvae, as shown by changes in Mn, Mw, and Mz or depolymerization. It was evident that LDPE depolymerized more rapidly than LLDPE and HDPE, and the extent of degradation appeared to be much more than that of HDPE and LLDPE (Table 1 and Figure S3A).

FTIR analyses showed formation of newly oxidative functional groups, i.e., stretching of C–O–C groups ($1100\text{--}1300\text{ cm}^{-1}$) carboxylic acids ($1708\text{--}1698\text{ cm}^{-1}$), ketones ($1723\text{--}1713\text{ cm}^{-1}$), aldehydes ($1740\text{--}1733\text{ cm}^{-1}$), and lactones ($1786\text{--}1780\text{ cm}^{-1}$) (Figure S3B). In this study, to better determine the degradation of the three PE MPs, the CI of a single sample was calculated (Table 1 and Fig. 1C). All virgin LDPE, LLDPE and HDPE show a high index after biodegradation by *T. obscurus* and *T. molitor* larvae. For PE MPs, a polymer backbone signal peak at 1471 cm^{-1} decreased in the FTIR spectra of the frass of both species and the incorporation of oxygen into the PE polymer chains due to oxidation (Figure S3B) (Peng et al., 2019; Yang et al., 2022). The CI of residual PE

Table 1Characterization of biodegradation of three PE in *T. molitor* and *T. obscurus* larvae after fed with PE for 21 days.

Item	Survival rate, %	Specific PE consumption rate ^a , mg PE • 100 larvae ⁻¹ •day ⁻¹	Residual PE in frass, %	Mn, kDa	Mw, kDa	Mz, kDa	CI ^b
LDPE D	91 ± 0.71	8.26 ± 0.28	52.23 ± 7.22	69.0 ± 2.6	162.4 ± 6.0	315.0 ± 10.2	16.49 ± 0.22
LLDPE D	88.13 ± 0.53	8.73 ± 0.19	59.17 ± 12.16	82.2 ± 3.1	193.5 ± 7.1	379.1 ± 13.2	6.62 ± 0.01
HDPE D	90 ± 2.83	8.04 ± 0.06	68.72 ± 8.96	80.8 ± 3.1	201.6 ± 8.1	415.5 ± 16.9	18.76 ± 0.16
WB D	88 ± 3.18	nd	nd	nd	nd	nd	nd
LDPE Y	81.38 ± 4.42	9.31 ± 0.35	51.82 ± 8.45	67.6 ± 3.0	158.9 ± 5.8	306.5 ± 11.3	12.05 ± 0.10
LLDPE Y	80.25 ± 0.35	8.03 ± 0.08	62.00 ± 5.25	71.6 ± 3.0	179.2 ± 6.9	361.1 ± 12.6	7.26 ± 0.01
HDPE Y	80.38 ± 3.71	7.68 ± 0.13	64.52 ± 14.65	77.4 ± 3.0	200.2 ± 7.7	404.6 ± 15.7	10.74 ± 0.09
WB Y	85.13 ± 0.18	nd	nd	nd	nd	nd	nd

Note: The initial larval number: 400. nd = not determined; the values represent mean ± SD, n = 3. The initial weight: *T. molitor* larvae, 27 ± 0.5 mg larva⁻¹; *T. obscurus* larvae, 130 ± 5.0 mg larva⁻¹.

^a Specific PE consumption was calculated on the basis of the mass of PE consumed over the test period (21 days) and the initial number of larvae.

^b CI = Carbonyl index, Virgin LDPE: 3.54 ± 0.07, Virgin LLDPE: 3.71 ± 0.16, and Virgin HDPE: 2.87 ± 0.01.

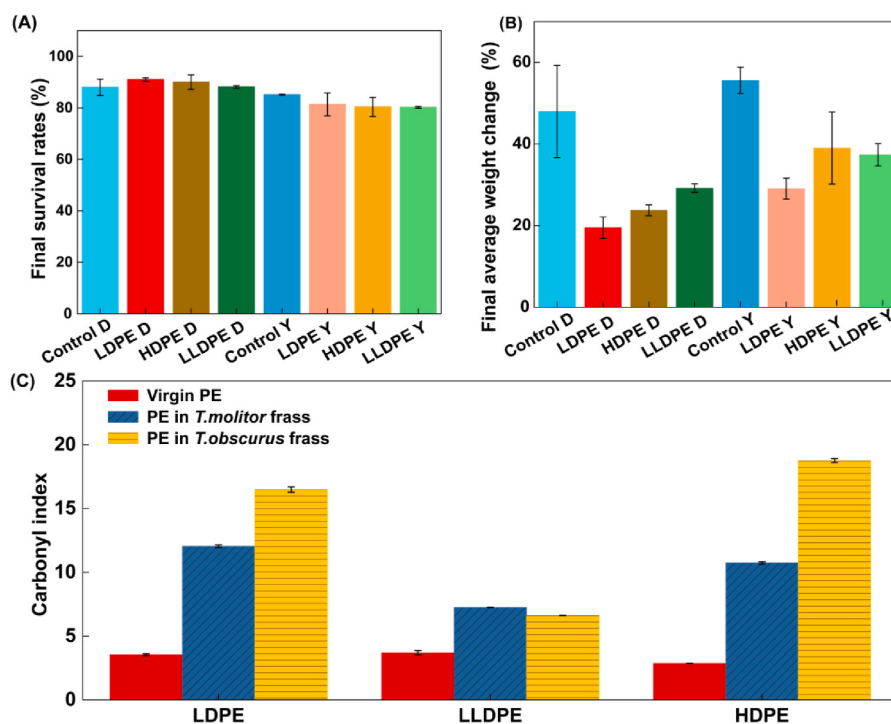


Fig. 1. Physiological responses of *T. molitor* and *T. obscurus* larvae fed with LDPE, HDPE, and LLDPE versus wheat bran. (A) Survival rates. (B) Weight changes. Comparison of (C) carbonyl index of residual PE polymers in the frass of *T. molitor* and *T. obscurus* fed respective virgin LLDPE, LDPE, and HDPE only. Y = Yellow mealworms (*T. molitor*); D = Dark (*T. obscurus*); Control: feeding wheat bran; Significance (Student's t-tests) p < 0.05 indicated by *, ns: no significance. (For interpretation of the references to colour in this figure legend, the reader is referred to the Web version of this article.)

MPs polymers from the frass of *T. obscurus* and *T. molitor* larvae fed with PE powders increased obviously (Table 1, p < 0.05), i.e., LDPE increased by 240.01 ± 6.65% and 365.40 ± 14.97%, HDPE increased by 274.62 ± 3.90% and 554.59 ± 5.87%, and LLDPE increased by 96.01 ± 8.10% and 78.94 ± 7.36%, respectively (Table 1 and Fig. 1C). Differences in the ability of both larvae to oxidize three different PE powders are similar to previously reported studies on the ability of *T. molitor* and *T. obscurus* to oxidize PS (Peng et al., 2019). In addition, ¹H NMR analysis further showed incorporation of oxygen (aminoic, carbonyl, aldehyde, methyl, and unsaturated allylic groups) and the breakdown of long chain PE polymers. Variations in ¹H NMR spectra between 1.4 and 1.7 ppm (Figure S3C) revealed that the frass samples from *T. molitor* groups had more extra peaks than those from *T. obscurus* groups. It implies that the two *Tenebrio* species' biodegradation processes are distinct from one another.

3.3. Organic compositions of the larvae

Tenebrio larvae are increasingly being recognized as effective tools for plastic degradation and a valuable protein source for both livestock and humans. In particular, the Cys content of *T. obscurus* is approximately 15.6-fold higher than that of *T. molitor* (Ding et al., 2023; Peng et al., 2023a). The nutritional composition of *T. obscurus* and *T. molitor* biomass is shown in Fig. 2 and Table 2. In terms of the total carbohydrate content of larvae at the end of the experimental period, no significant differences were observed in *T. obscurus* groups. The larvae fed with LDPE had the highest total carbohydrate content (5.2 ± 0.55%), which was significantly higher than the larvae fed with HDPE (3.88 ± 0.54%) or LLDPE (3.56 ± 0.39%) (p < 0.05), with all PE fed *T. molitor* groups having a significantly higher carbohydrate content than the WB fed group (2.45 ± 0.18%). Furthermore, under normal dietary conditions (WB-fed), the carbohydrate content of *T. obscurus* (3.34 ± 0.17%) was obviously higher than that of *T. molitor* (p < 0.05), while the opposite

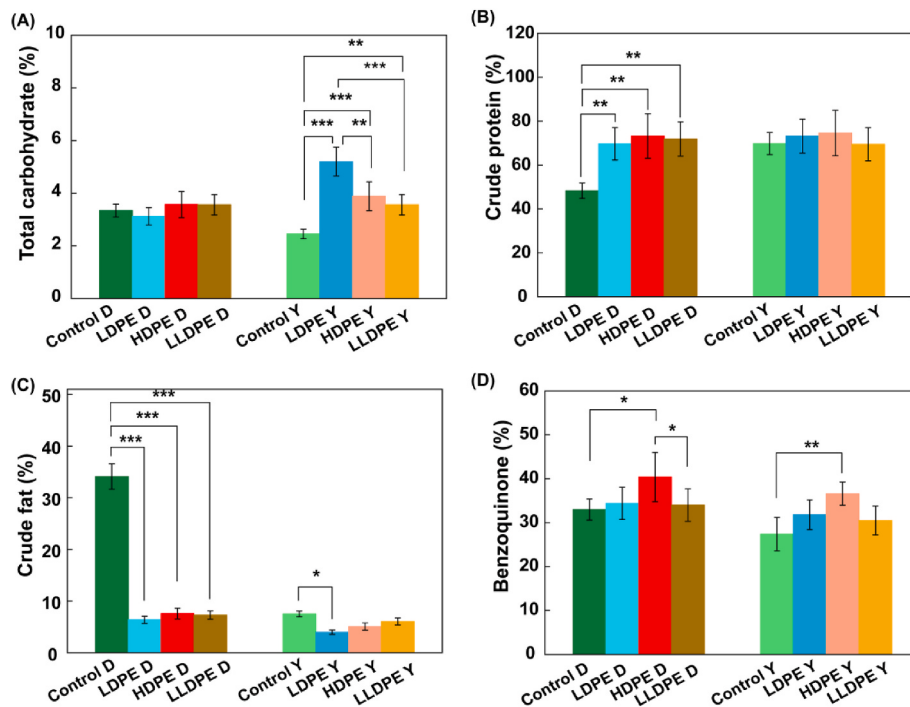


Fig. 2. Biomass composition of *T. molitor* and *T. obscurus* larvae fed with LDPE, HDPE, and LLDPE versus wheat bran at the end of the test (21 days): total carbohydrate (A), crude protein (B) crude fat (C) and benzoquinone (D). Y = Yellow mealworms (*T. molitor*); D = Dark (*T. obscurus*); Control: feeding wheat bran; Significance (Student's t-tests) $p < 0.05$ indicated by *, ns: no significance. (For interpretation of the references to colour in this figure legend, the reader is referred to the Web version of this article.)

Table 2
Comparison of fatty acid composition (%) in the dry biomass of mealworm.

Item	C12:0	C14:0	C16:1 Δ -9	Palmitic acid	C17:0	linoleic acid	Oleic acid	C18:0
LDPED	nd	nd	0.05 ± 0.01	1.23 ± 0.09	0.01 ± 0	1.44 ± 0.11	3.3 ± 0.23	0.35 ± 0.03
LLDPED	nd	0.23 ± 0.01	0.08 ± 0.01	0.98 ± 0.1	0.02 ± 0.01	1.94 ± 0.14	3.69 ± 0.18	0.35 ± 0.03
HDPED	nd	nd	0.06 ± 0.01	2.82 ± 0.16	nd	1.13 ± 0.08	2.98 ± 0.2	0.64 ± 0.04
WB D	nd	1.61 ± 0.05	0.37 ± 0.02	6.48 ± 0.34	nd	6.56 ± 0.42	18.31 ± 1.33	0.73 ± 0.05
LDPEY	1.06 ± 0.06	0.24 ± 0.03	0.08 ± 0.02	0.6 ± 0.03	0.01 ± 0.01	0.74 ± 0.06	1.1 ± 0.09	0.17 ± 0.02
LLDPEY	0.02 ± 0	0.14 ± 0.02	0.06 ± 0.01	0.65 ± 0.04	0.01 ± 0.01	1.65 ± 0.1	3.27 ± 0.29	0.24 ± 0.03
HDPEY	1.41 ± 0.11	0.33 ± 0.06	0.1 ± 0.03	0.77 ± 0.04	0.01 ± 0.01	0.89 ± 0.05	1.36 ± 0.08	1 ± 0.1
WBY	1.44 ± 0.13	0.4 ± 0.04	0.14 ± 0.03	1.14 ± 0.05	0.02 ± 0.01	1.86 ± 0.21	2.16 ± 0.13	0.35 ± 0.05

Note: nd = not determined; the values represent mean ± SD, n = 3.

was observed under PE-fed conditions (Fig. 2A and S4.A). The analysis of crude protein and crude fat composition of *T. obscurus* fed with PE-MPs and WB-fed larvae, showed that all PE-fed larvae exhibited a significantly higher crude protein content and lower fat content than WB-fed larvae ($p < 0.05$, Fig. 2B and S4.B). A similar phenomenon was observed in *T. molitor* groups. Interestingly, the crude protein content of *T. obscurus* was obviously lower than that of *T. molitor* under normal dietary conditions and PE-diet conditions, although the biomass protein content of both species was comparable. However, the Cys content of *T. obscurus* was clearly higher than that of *T. molitor*, under both dietary conditions (Fig. S5). Previous research has demonstrated that the protein and fat content of the diet have an impact on the protein, fat, and fatty acid content of *Tenebrio* larvae (van Broekhoven et al., 2015). After the 21-day test period, WB-D exhibited an approximately five-fold higher crude fat content than *T. obscurus* in the PE-fed groups, while the crude fat content of WB-Y was higher than that of larvae in the (LD/HD/LLD)PE-Y group (Fig. 2C). *T. obscurus* larvae consistently maintained a higher crude fat content than *T. molitor*. A total of 8 fatty acids were detected in all groups, with the fatty acid types being more abundant in all *T. molitor* groups and no lauric acid (C12:0) detected in any *T. obscurus* groups. The predominant fatty acids in all eight exposure

groups for both species were palmitic acid, oleic acid and linoleic acid, accounting for 59–94% of the total fatty acids (Table 2). The proportion of unsaturated fatty acids (palmitoleic acid (C16:1 Δ -9), oleic acid and linoleic acid) varied from 46% to 83%. The HDPE groups had the lowest proportion of unsaturated fatty acids, with 55.22% in HDPE-D and 46.19% in HDPE-Y. The LDPE-D group had a similar unsaturated fatty acid content (74.99%) to the WB-D group (74%). The LDPE-fed larvae had the highest content of unsaturated fatty acids (LDPE-D: 78.44% and LLDPE-Y: 82.18%) among all PE diet-fed groups. Previous studies have shown that unsaturated fatty acids impact and regulate membrane formation, fluidity, and intercellular communication in larvae (Al-Beloshei et al., 2015; Nicol et al., 2018; Suppiger et al., 2016).

Additionally, the physiological response of larvae to different PE diets varies. In this study, it was found that *Tenebrio* larvae have higher levels of benzoquinone, an important defense molecule, with the highest levels occurring in the HDPE-fed group. The results were statistically significant ($p < 0.05$; Fig. 2D and S4.D). This increase may be due to the impact of the PE diet, which increases the burden on the larval gut and subsequently induces a physiological response in the larvae. Both species of *Tenebrio* larvae had difficulty obtaining energy and nutrients from their diet when fed with HDPE. This difficulty is likely due to the lower

degree of carbon chain branching and higher crystallinity of HDPE (Yang et al., 2022), which triggers a higher level of benzoquinone secretion by the larvae. Similar to formic acid secreted by ants and venom secreted by bees, quinone-like substances are important extracellular defence molecules in the secretion of Tenebrionidae. For example, the 1,4-benzoquinone (Sahu et al., 2023) plays a role in defending against predators and pathogenic microorganisms. Tenebrionidae can also regulate the secretion of quinone based on environmental factors such as diet (Yezerski et al., 2004). In this study, a higher level of benzoquinone was detected in the *T. obscurus* larvae, which is related to their diet composition and the influence of the insect source. Among the larvae, the highest level of benzoquinone was found in the HDPE feeding group, showing a significant increase compared to the WB feeding group ($p < 0.05$; Fig. 2. D and S4. D). The effects of a PE diet may have contributed to the increased burden on the larval gut, subsequently triggering the larvae's immune physiological response. Obtaining energy and nutrients from diets on HDPE is particularly challenging for larvae due to the lower degree of branching in the carbon chain and higher crystallinity of

HDPE (Yang et al., 2022), which triggers the larvae to secrete more quinones to avoid being cannibalized. Studies have shown that this process does not reduce the lifespan and reproductive capacity of the mealworms. In other words, the increase in benzoquinone secretion by *T. molitor* and *T. obscurus* during the process of feeding on degraded plastics represents the optimal balance and investment in resource allocation in vivo between external immune defence, growth and development, or energy acquisition strategies (Joop et al., 2014).

3.4. Gut microbial community diversity and shift

16S rRNA gene sequencing was used to examine the gut microbiomes of both *Tenebrio* species fed respective three PE polymers (Figs. 3 and 4). The Simpson and Heip evenness diversity index values showed significant variation among all eight groups, with HDPE-fed larvae being less even, presumably due to the presence of dominant taxons (Fig. 3. A and S6). According to the Levins OTU abundance matrix, the niche breadth indicates the interactions of OTUs with their environment. The results

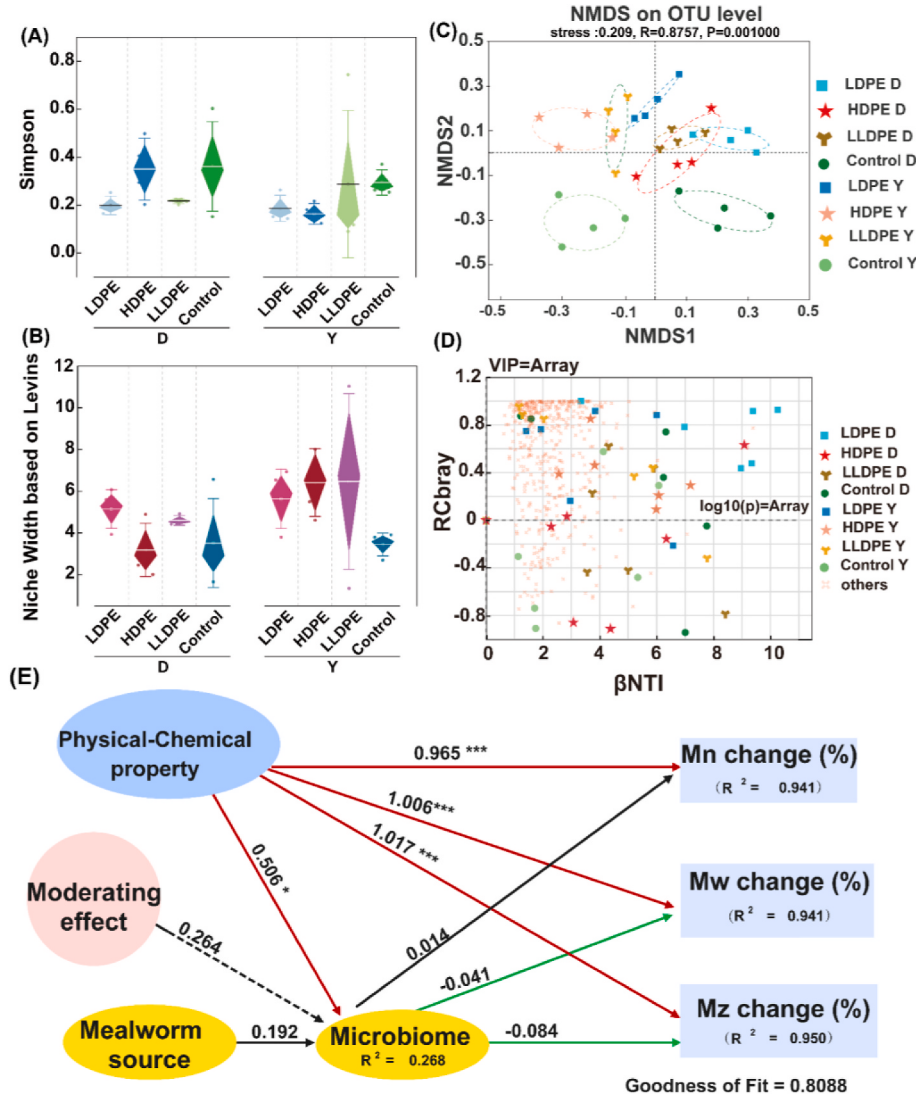


Fig. 3. The assembly of the gut microbial communities of *T. molitor* and *T. obscurus* larvae fed with LDPE, HDPE, LLDPE versus wheat bran (WB). (A) Bacterial diversity analyses based on 16S rRNA gene amplicons of OTUs from *T. molitor* and *T. obscurus* larvae. (B) Niche width analyses based on Levins of the two *Tenebrio* species. (C) β diversity analyses based on the OTUs level of the both species. (D) Microbial community assembly or community structure by β NTI/RCbray. (E) Effects of three major variables on the gut communities and molecular weight changes based on partial least squares path modeling. The red arrows represent positive pathways and the green arrows indicate negative pathways. The standard path coefficients are shown on the arrow. GOF = good of fitness. Mn = number averaged molecular weight; Mw = weight averaged molecular weight; Mz = size averaged molecular weight; WCA = water contact angles. Samples were collected on day 21. (For interpretation of the references to colour in this figure legend, the reader is referred to the Web version of this article.)

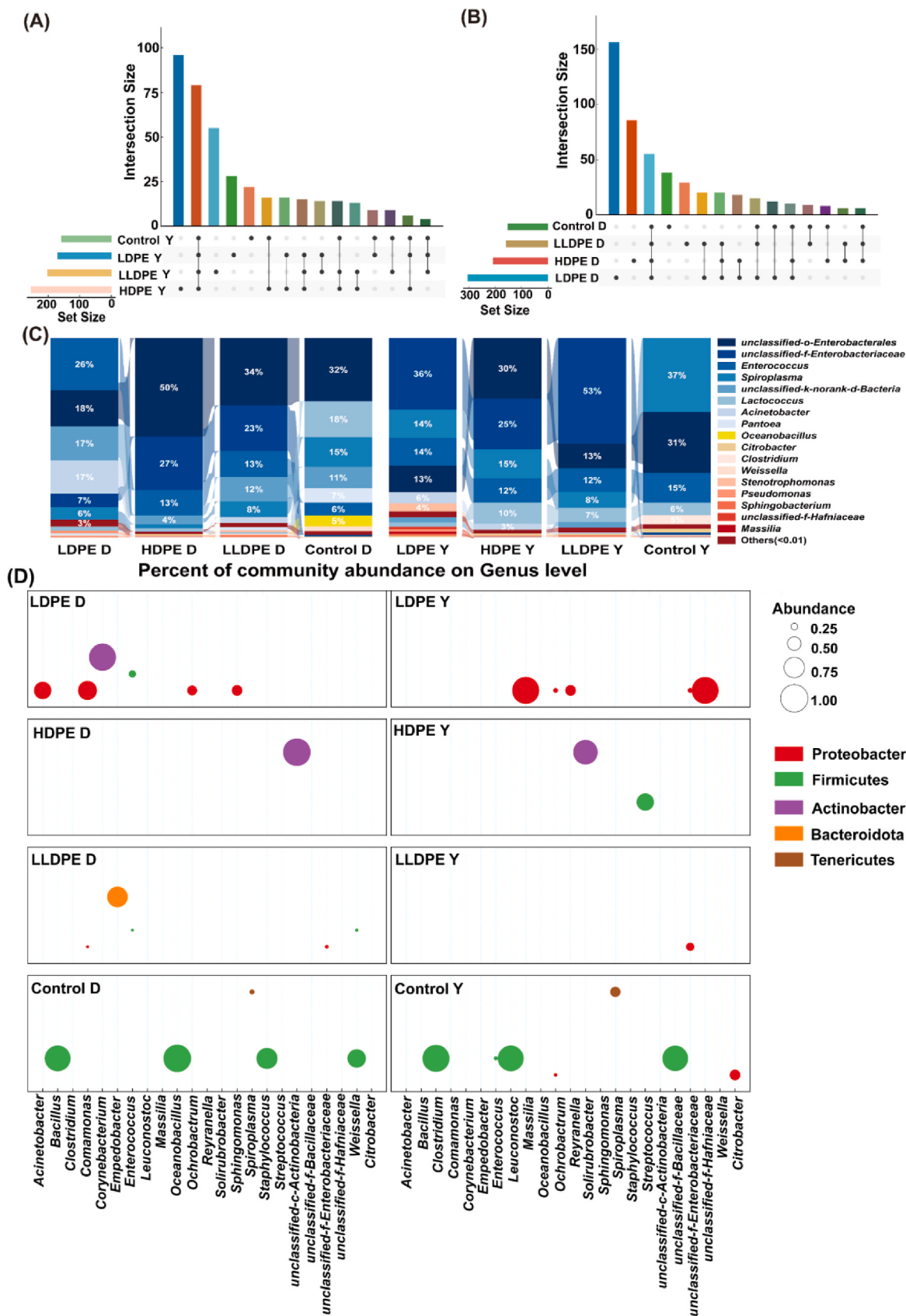


Fig. 4. Gut microbial community succession of *T. molitor* and *T. obscurus* larvae fed with LDPE, HDPE, LLDPE versus wheat bran (WB). (A–B) Analysis of the variability of OTU between *T. molitor* versus *T. obscurus* groups by Venn. (C) Relative bacterial abundances of dominant genus (top 20) in the gut microbiomes of *T. obscurus* and *T. molitor* larvae fed different diets. (D) Microbial indicator taxa for different diets of *T. obscurus* and *T. molitor*. Indicator genera were identified with the indicator value analysis (IndVal). Each dot represents a unique genus.

show that the intestinal flora of PE-fed mealworms was more generalized compared to that of the control groups (Fig. 3. B). A significant dissimilarity in microbial communities based on diet and species was evident through a PERMANOVA analysis utilizing Bray-Curtis dissimilarity ($p = 0.001$) (Fig. S7, Table S4).

The microbiomes of the larvae that were fed PE or WB diets exhibited distinct clusters for PE-fed and WB-fed larvae (Fig. 3. C and S8-9). In summary, feeding with PE-MPs enhanced diversity and changed the niche width of the larval gut microbiomes in both species (Luo et al., 2021). The niche widths of all PE-MP fed groups were higher than that of the WB group. The abundance of gut microbe species and ecological interactions within the gut communities in both *Tenebrio* species were affected by the varying nutrient supplies provided by LDPE, HDPE, LLDPE, and WB. High-nutrient environments can enhance competition between species in natural bacterial communities where collaboration and competition are prevalent (Dai et al., 2022; Engel and Moran, 2013; Nyholm and Graf, 2012; Palmer and Foster, 2022).

PE is a carbon-rich oligotrophic substance without any nitrogen source. The intestinal flora of *Tenebrio* larvae exhibited a strong capacity to adapt when larvae were fed PE-MPs as an energy and carbon source. Feeding with a PE diet likely added a selection pressure on the larvae due to their additional nutrient requirements, e.g., nitrogen source, leading to the development of a new microbiome adapted to a N-deficient environment (Fig. 3). This selection pressure adaptation resulted in the reduction of functional redundancy and an increase in resource utilization efficiency within the community. Another recent study by our team confirmed that when both species of mealworms consumed LDPE foam supplemented with their traditional diet, the gut flora with plastic-degrading functions played a more important role. However, nitrogen fixation by the gut flora, which was supplemented as a source of nitrogen, was diminished (Ding et al., 2023), while, the study did not fully assess changes in biomass (fat, carbohydrate, protein, etc.) and oxidative stress in larvae on different diets.

3.5. Microbial community composition and sensitivity

The assembly and structure of microbial communities depend on a combination of stochastic and deterministic ecological processes. Understanding gut microbial diversity and function requires consideration of these processes (Dini-Andreote et al., 2015; Jiao et al., 2020; Stegen et al., 2013; Tripathi et al., 2018). The degree of “heterogeneous selection” within the gut communities of all eight groups (LDPE-Y, LLDPE-Y, HDPE-Y, WB-Y, LDPE-D, LLDPE-D, HDPE-D and WB-D) was found to be 68% in this study. Subsequently, RCBay was used to further partition the pairwise comparisons that were not assigned to selection ($|\beta\text{NTI}| < 2$). Here the fractions of all pairwise comparisons, with $|\beta\text{NTI}| < 2$ and $|\text{RCBay}| < 0.95$, were used to estimate the influence of “undominated” assembly. In this study, the overall estimated influence of “undominated” assembly was 26%, which mostly consisted of weak selection, weak dispersal, diversification and/or drift. Finally, the assembly with $\text{RCBay} > 0.95$ was considered to have ‘dispersal limitation’ and was estimated to be 6% (Fig. 3. D). Deterministic ecological processes had a higher influence (68%) than stochastic ecological processes, suggesting that microbial communities were mostly influenced by the host diet and species, or were not the result of a single dominant process (i.e., ‘undominated’ assembly).

The sensitivity of the gut microbiomes was assessed by comparing their responses to variables including host-specificity (*Tenebrio* species) and PCPs of PE-MPs (WCAs, PE type, Mn, Mw, Mz and crystallinity degree) (Fig. 3. E and S9-11, Tables S3–6). The compositional variability of the larval gut microbiome ($n = 32$) was significantly explained by *Tenebrio* species, based on dbRDA using a permutational ANOVA and VPA (Fig. S9, Table S5).

Overall, the PCPs of PE-MPs caused significant compositional variation (Tables S3 and 6 and Fig. 3. E). Analysis of the gut microbiome using PLS-SEM revealed both direct and indirect effects of host-

specificity (*Tenebrio* species) and the PCPs of PE-MPs on the microbiomes in both species, leading to depolymerization (Fig. 3. E and Table S6). The gut microbiome determines the change in PE molecular weight (Mw, Mn and Mz) or pathway of PE degradation. The path coefficients of the PCPs of PE-MPs were the highest, with the molecular weight of the original PE being the most influential among all tested properties. Molecular branching, weight distribution, and crystallinity degree followed, all of which had path coefficients greater than 0.9. The abundances of *Acinetobacter*, *Pseudomonas*, *Achromobacter*, *Ralstonia*, *Glutamicibacter*, *Delftia*, *Ochrobactrum*, *Sphingomonas*, *Micromonas* and *Staphylococcus* were significantly associated with factors influencing gut microbiome assembly ($p < 0.05$) and exhibited higher path coefficients (Fig. 3. E and S10). Overall, the goodness of fit (GOF) for *Tenebrio* species and PCPs of PE-MPs was 0.8088. Despite the model’s relatively high predictive power, these findings suggest that there is still some unexplained variation, which is consistent with the VPA results.

Community similarity was assessed using Venn diagram analysis based on OTUs. The OTUs from all eight groups were compared (Fig. S11), revealing differences in the number of independent OTUs in different groups. 44 OTUs were shared between all groups, while 79 were shared only between *T. molitor* groups (Fig. 4. A) and 55 were shared only between *T. obscurus* groups (Fig. 4. B). For both *T. obscurus* and *T. molitor* groups, the number of shared OTUs in larvae fed with LDPE and LLDPE was higher than the number of shared OTUs in larvae fed with LDPE and HDPE or LLDPE and HDPE (Fig. 4. A and B). At the genus level, *Unclassified-o-Enterobacteriales*, *unclassified-f-Enterobacteriaceae*, *Enterococcus* and *Spiroplasma* were the most common gut flora detected in both *Tenebrio* species across all treatments (Fig. 4. C). The relative abundances of these genera were lower in the WB-fed groups compared to the PE-fed groups. *Acinetobacter* was only present in the PE-fed groups of both *Tenebrio* species, with a stable relative abundance across all PE-fed *T. molitor* groups (LDPE: 6%, HDPE: 3%, and LLDPE: 1%), regardless of the PE-MPs PCPs. *Stenotrophomonas* were present in the LLDPE-D, LDPE-Y, and LLDPE-Y groups but were absent in the WB-fed larvae. Furthermore, the presence of *Lactococcus*, *Spiroplasma*, *Citrobacter*, *Clostridium*, *Pseudomonas*, *Sphingomonas*, *unclassified-f-Hafniaeae*, and *Massilia* was observed in all PE-fed groups, but not in the WB-fed control groups. Therefore, based on taxonomic grouping, the microorganisms that specifically increased in the larval gut microbiomes were upregulated due to dietary conditions. The larvae of *T. obscurus* contained a richer variety and high abundance of microorganisms related to nitrogen metabolism, i.e., *Comamonas*, *Citrobacter*, *Actinobacteria* (*unclassified-c-Actinobacteria* and *Corynebacterium*) (Chang et al., 2022), *Acinetobacter*, *Ochrobactrum*, *Reyranella* (Xue et al., 2020), *Enterococcus*, *Empedobacter* (Mavriou et al., 2021), *Oceanobacillus*, *Bacillus* and *Spiroplasma* (Ding et al., 2023; Yang et al., 2023a). In contrast, *Massilia* (Balazs et al., 2021), *Reyranella*, *unclassified-f-Enterobacteriaceae* (Kampfer et al., 2005), *Ochrobactrum*, *Solirubrobacter* (Zhang and Zhao, 2019), *Clostridium*, *Leuconostoc* (Martinez-Rodriguez et al., 2014), *Unclassified-f-Bacillaceae*, *Citrobacter*, *Spiroplasma*, *Enterococcus* and *Ochrobactrum* were the functional nitrogen metabolism-associated microbes in *T. molitor* groups. These microorganisms are important because they can provide nitrogen for larvae in nitrogen-deficient feeding conditions.

Based on the observed changes in gut microbiome according to diet and host-specificity, the ability to infer gut microbiome state using microbial community data and indicator species (specific gut microbes upregulated due to diet or PE PCPs in *Tenebrio* larvae) was determined using indicator value analysis (Glasl et al., 2019) (Fig. 4. C). The indicator value of each genera was based on its sensitivity to dietary state, which was calculated using the frequency and abundance of genera in all eight groups. In total, 22 genera were identified as being significant indicators which were present in all eight groups ($p < 0.05$). Microbial genus assemblages that were indicative of PE type and *Tenebrio* species (based on group averages) appeared to accompany the experimental period. Furthermore, the study identified 5 indicator genera were

identified for Control-D related phyla Tenericutes and Firmicutes, while 7 indicator genera were identified for Control-Y, belonging to Tenericutes, Proteobacteria and Firmicutes (Fig. 4. C). The number of indicator genera was highest in the larvae fed LDPE compared to other PE-fed groups. The LDPE-Y group had 5 indicator genera identified, which belonged to Proteobacteria (*Massilia*, *Ochrobactrum*, *Reyranella*, *unclassified-f-Enterobacteriaceae* and *unclassified-f-Hafniaceae*). Meanwhile in the LDPE-D group, 6 indicator genera were identified, which belonged to Actinobacteria (*Corynebacterium*), Proteobacteria (*Acinetobacter*, *Comamonas*, *Ochrobactrum* and *Sphingomonas*) and Firmicutes (*Enterococcus*). *Unclassified-c-Actinobacteria* belonging to Actinobacteria was a unique indicator identified for the HDPE-D group, while Actinobacteria (*Solirubrobacter*) and Firmicutes (*Streptococcus*) had significant indicator values in the HDPE-Y group ($p < 0.05$). In LLDPE-fed groups, *Empedobacter* belonging to Bacteroidota was found to be an important indicator in the LLDPE-D group, while *unclassified-f-Enterobacteriaceae* (Proteobacteria) was significantly associated with the LLDPE-Y group. Overall, the gut microbiome of larvae on the PE diet contained 22 indicators related to nitrogen metabolism, including *Comamonas*, *Ochrobactrum*, *Reyranella*, *Enterococcus*, *unclassified-f-enterobacteriaceae*,

Solirubrobacter, and *Citrobacter*. Additionally, Actinobacteria were more strongly correlated in both *Tenebrio* species with the ingestion and biodegradation of HDPE MPs than LDPE MPs and LLDPE MPs.

3.6. Functional features of the gut microbiome

This study identified differences in the intestinal microbial ecology, metabolic pathways and microbial function of larvae fed with HDPE, LLDPE, LDPE or WB diets, were identified using the Functional Annotation of Prokaryotic Taxa (FAPROTAX) (Fig. S12). Both *Tenebrio* larvae showed enhanced gut microbiome functions associated with carbon and nitrogen metabolism after ingesting PE. These metabolic activities are crucial for plastic degradation by the larvae, as the plastic diet does not provide a nitrogen source for mealworms during the degradation of Nitrogen-free and carbon-rich PE polymer powders. These metabolic activities are crucial for plastic degradation by the larvae, as the plastic diet does not provide a nitrogen source for mealworms during the degradation of Nitrogen-free and carbon-rich PE polymer powders. Nitrogen is an essential element for protein and nucleic acid synthesis, as well as growth metabolism in insects. The gut microbiota of insects has

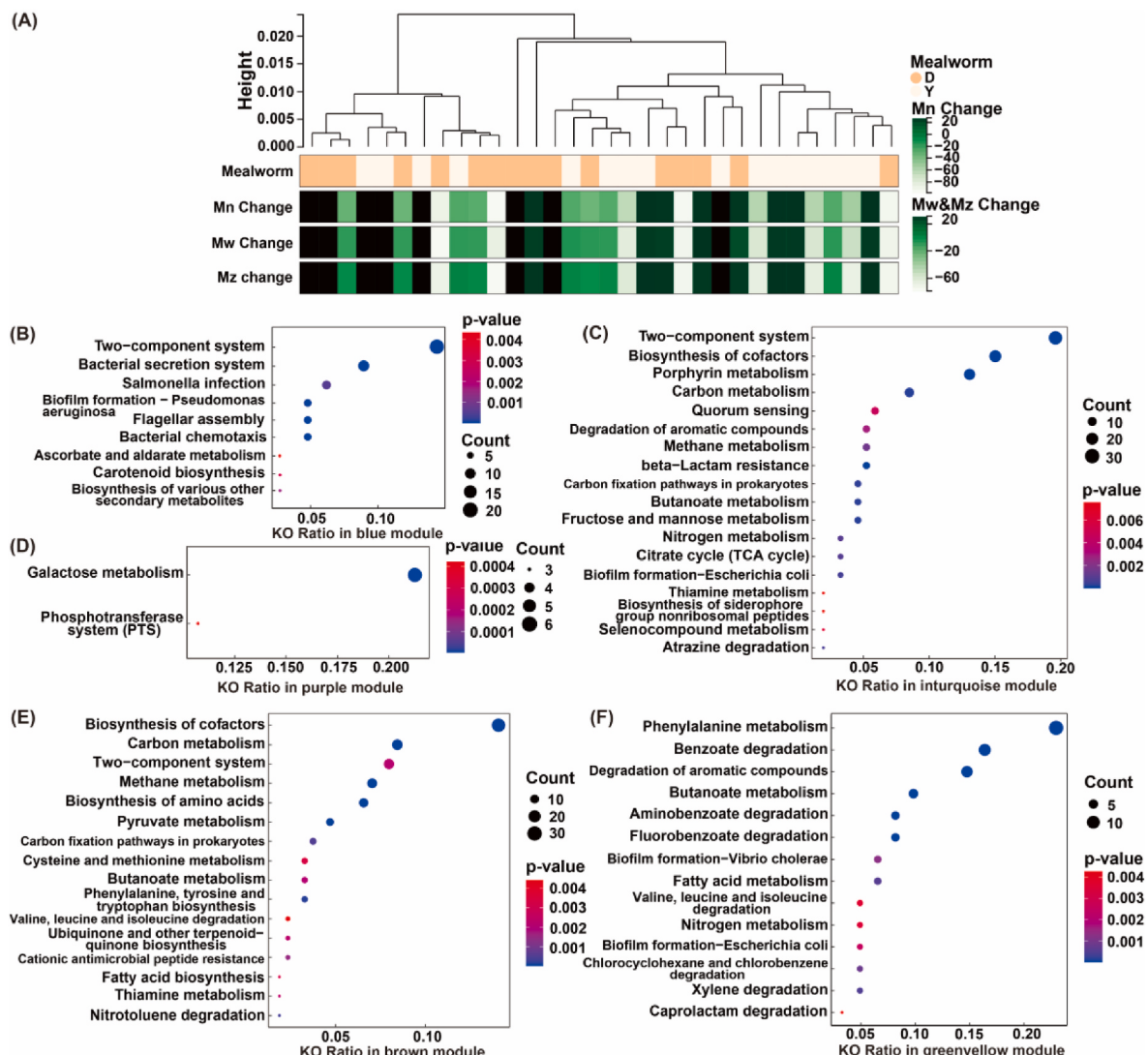


Fig. 5. KO enrichment analysis was based on WGCNA. (A) All the samples were in the clusters, all samples passed the cuts. Module-based enrichment analysis of gut bacterial KO in respective diet groups: KO modules highly associated with *T. obscurus* in the blue module (B), KO modules highly associated with *T. molitor* in the turquoise module (C). KO modules highly associated with molecular weight (M_n , M_w and M_z) change in the purple (D), brown (E) and greenyellow (F) modules. M_n = number averaged molecular weight; M_w = weight averaged molecular weight; M_z = size averaged molecular weight. (For interpretation of the references to colour in this figure legend, the reader is referred to the Web version of this article.)

the potential to fix nitrogen biologically, which helps to maintain their nitrogen nutrition to a certain extent. Compared to a PE diet, the nitrogen nutrition in a wheat bran diet can largely meet the nitrogen requirements. This is evident in the following functions: aerobic chemoheterotrophy, nitrate respiration, nitrite respiration, nitrous oxide denitrification and denitrification, with the observed increase in function being significant for *T. obscurus* larvae according to the Wilcoxon rank-sum test ($p < 0.05$). *T. molitor* larvae fed with PE-MPs exhibited a significant increase in aromatic compound degradation as compared to the WB fed group ($p < 0.05$), although chitinolysis was only significantly increased in the HDPE-Y group. This finding indicates that the *Tenebrio* gut flora adapted to the PE diet, by enhancing a variety of carbon and nitrogen metabolism processes. Carbon and nitrogen metabolism-associated ecological functions were richer and more significantly enhanced in *T. obscurus* than in *T. molitor*, possibly in order to balance higher protein requirements (Fig. 2, B and S4.B) (Peng et al., 2019). Under nitrogen-deficient conditions, aromatic compound degradation and chitinolysis played a more important role than aerobic chemoheterotrophy, nitrite respiration, nitrate respiration, nitrous oxide denitrification, or denitrification for *T. molitor*, indicating that *T. molitor* larvae preferred to assimilate chitin-rich exoskeletons to obtain nitrogen.

KO numbers are assigned genes based on the encoded function (Kanehisa et al., 2017) and the expression values of 8073 KOs from 32 larvae samples were used to build the co-expression module (see Fig. 5, A for cluster analysis results). The power value mainly influences the independence and average degree of connectivity of co-expression modules and when the value was 20, the independence degree reached 0.86 and the average connectivity degree reached 59.51. Overall, 11 distinct KO co-expression modules were obtained from the larval gut microbiome analyses, ranging from large to small according to the number of genes included. Interactions of the 11 co-expression modules were analyzed and eigengene dendrogram and heatmap analysis were used to distinguish between the groups of correlated eigen-genes. The blue modules in the dendrogram were closely related to the function of gut flora during plastic degradation in *T. obscurus*, while turquoise was related to *T. molitor*. Three modules (purple, brown and green-yellow) were significantly associated with changes in Mw, Mn and

Mz (Fig. S13). The results of enrichment analysis for the identified modules show that a two-component system closely correlated with significant changes in the M_w, M_n and M_z of PE in both *Tenebrio* larvae (Fig. 5 B-F). This suggests that during the ingestion of PE, a two-component system is stimulated in larval gut flora to respond to the signal transduction and bacterial chemotaxis of different diets, leading to PE biodegradation. Furthermore, the significant enrichment of metabolic functions associated with energy and nutrient reserves further confirmed the observed transformation of fatty acids in all test larvae under different dietary conditions. This not only ensures the reproductive metabolism of microorganisms, but also promotes the biodegradation of persistent organics such as PE (Gao et al., 2016; Xue et al., 2023).

3.7. Oxidation stress and ecotoxicity

After continuous feeding with PE-MPs powder for 21 days, the biochemical indices associated with oxidative stress were investigated, to determine whether they were induced by the ingestion and degradation of different PE types in *T. obscurus* and *T. molitor*. Among these, reduced enzyme synthesis altered assembly of enzyme subunits or even enzyme inactivation may lead to oxidative stress in larvae. SOD is an activated antioxidant enzyme that can scavenge excess peroxidative free radicals (Chen et al., 2020). T-AOC reflects the organism's overall level of protection against oxidative stress damage caused by reactive oxygen species (ROS). The results showed that SOD and T-AOC contents of PE-fed mealworms showed a similar trend in both species: HDPE-Y/D > LLDPE-Y/D or LDPE-Y/D > Control-Y/D (Fig. 6 A-B). The MDA content of larvae was also monitored to determine oxidative damage to membrane lipids (Peng et al., 2019), showing that the MDA content of larvae in all PE-fed groups was higher than in the WB-fed group. However, the MDA content trend varied according to species. *T. molitor* exhibited a 2-to 3-fold higher MDA content in PE-fed groups than in the WB group, with the highest content of 4.99 ± 0.62 nmol/g fresh weight observed in the LDPE-Y group, followed by HDPE-Y, LDPE-Y and Control-Y. In *T. obscurus*, the MDA contents were ranked in the order: LLDPE-D (5.51 \pm 0.68) > LDPE-D (5.11 \pm 0.49) > HDPE-D (4.36 \pm 1.47) > Control-D (4.06 \pm 0.60) nmol/g fresh weight. These results suggest that the PE of both larval species fed on different PCPs stimulates the antioxidant

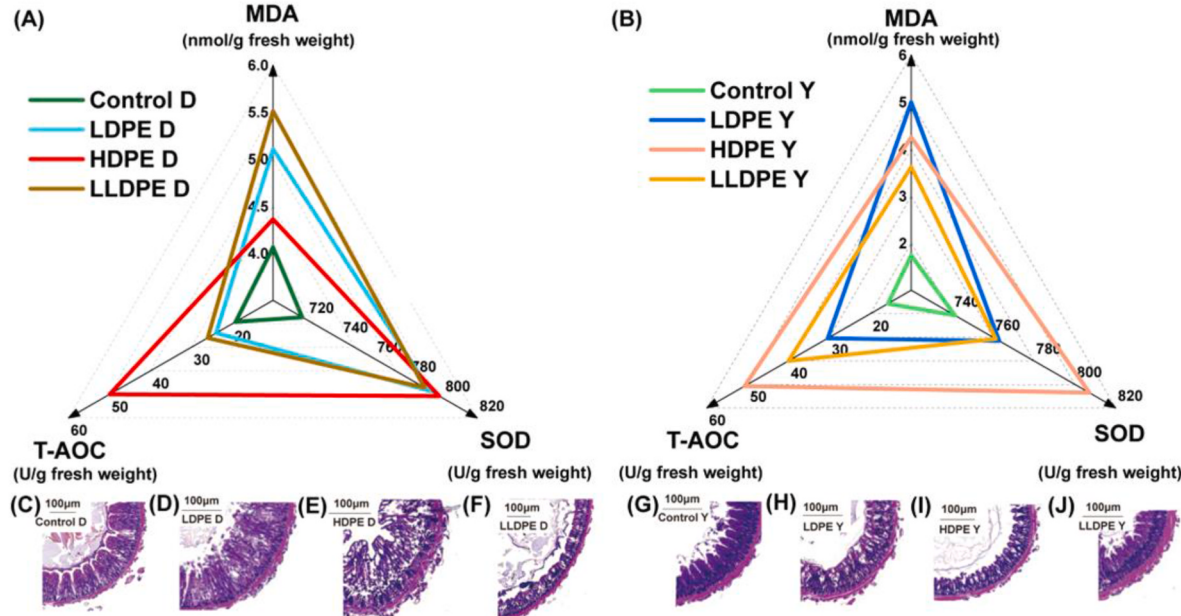


Fig. 6. Characterizations of the levels of oxidative stress pathological observation in mealworms after biodegradation of LDPE, HDPE, LLDPE MPs versus wheat bran. The levels of Total antioxidant capacity (T-AOC, nmol/g fresh weight), superoxide dismutase (SOD, U/g fresh weight) and malondialdehyde (MDA, nmol/g fresh weight) in (A) *T. obscurus* and (B) *T. molitor* at the end of the test (day 21). Midgut pathological observation of *T. obscurus* (C-F) and *T. molitor* (G-J).

capacity of the larval organism to cope with the survival stress caused by the diet. Simultaneous mitigation of different PE PCPs induced different degrees of oxidative stress and lipid peroxidation, which is consistent with previously reported results of MP-induced oxidative damage during plastic biodegradation in invertebrates (Li et al., 2021; Peng et al., 2022). The higher levels of SOD and T-AOC in the HDPE group indicated the stronger antioxidant capacity of both larvae under this dietary condition. It may be that HDPE with higher crystallinity and hardness aggravates intestinal tissue damage and stimulates the self-protection mechanism of the worms to secrete more antioxidant factors. MDA is a stable product of lipid peroxidation and its content decreases when ROS are removed by reaction with antioxidant enzymes (substances) (Chen et al., 2020). In this study, the MDA content in the HDPE group was not the highest among all the groups as expected, which may be due to the inhibition of lipid peroxidation by higher antioxidant capacity. In addition, increasing the dose of microplastic exposure may also induce changes in the antioxidant capacity of earthworms (*Eisenia fetida*), zebrafish (*Danio rerio*) and other organisms (Chen et al., 2020; Lei et al., 2018). The highest MDA levels in *T. obscurus* that ate LLDPE and *T. molitor* that ate LDPE in the present study may be caused by their higher PE consumption.

To further characterize the oxidation stress triggered by PE-MPs, larval gut health must be comprehensively evaluated. The midgut is an important organ for PE digestion, biodegradation, and immunity (Li et al., 2021; Magalhaes et al., 2007), with the health of the intestine heavily depending on the barriers provided by the intestinal mucosa, epithelial cells, inflammatory response, and parasitic microbiota (Baeckhed et al., 2005; Li et al., 2021). As shown in Fig. 6. C-J, damage to the intestinal structure was observed in all PE-fed larvae, which may be the result of mechanical damage caused by the rough PE surface, as particles tend to aggregate in the digestive tract and squeeze the epithelial cells. This effect was observed most prominently in the HDPE-Y/D group larvae fed on the more crystalline virgin HDPE powder, which exacerbated mechanical damage to the larval gut. Therefore, gut damage could be responsible for the observed differences in oxidative stress parameters and lower SRs caused by PE-MPs. The predictive results of toxicity estimation via the consensus method in T.E.S.T. showed that most of the degradation products and intermediates induced developmental toxicity, except for three compounds that were not included in the database (LDPE-Y: 100%, HD/LLDPE-Y: 85.71%, LDPE-D: 75%, HDPE-D: 83.33% and LLDPE-D: 76.92%). Based on these results, the degradation products of PE-fed *T. molitor* were considered highly likely to induce developmental toxicity, which was consistent with the low SRs observed. Among all the compounds identified in frass from PE-fed groups, no substances were recorded as being toxic in the *Daphnia magna* LC₅₀ (48 h) database (Table S7). In contrast, the Oral rat LD₅₀ of C₂H₄O₂ (CAS: 64-19-7) for rats was 3308.15 mg/kg, while LLDPE degradation intermediates exhibited a higher LD₅₀ (3467.62 mg/kg). This provides a valuable reference for assessments of the eco-toxic effects of plastic degradation products. Future studies should investigate the toxic effects of biodegradation compounds and intermediates generated by different plastic types such as PS, PP and PVC. Furthermore, toxicity experiments (vertebrates and invertebrates) should be conducted to further assess the ecological effects of plastic degradation processes and to help develop safe biological treatments for different plastic types.

4. Conclusion and implication

This study reported the effects of three distinct polyethylene (PE) polymers i.e., LDPE, HDPE and LLDPE on the gut microbiome, oxidative stress, and ecotoxicity after two major plastic-degrading *Tenebrio* larvae, *T. obscurus* and *T. molitor*, received these polymers as diets. Both *T. obscurus* and *T. molitor* larvae effectively biodegraded the three PE polymers via symbiotic reactions by the host larvae and gut microbiota. Both *T. molitor* and *T. obscurus* larvae biodegraded the three PE polymers

effectively as a sequence of LDPE > LLDPE > HDPE. However, physiological response and larval biomass developed were slightly different due to larval speciation.

Distinct differences in microbial diversities and gut microbial composition were observed among the two insect species and three PE polymers compared with WB-fed controls. *T. molitor* and *T. obscurus* larvae showed different oxidative stress responses and eco-toxicity to the three PE polymers. In general, the negative responses followed the order of HDPE > LLDPE > LDPE. *Actinobacteria* played an important role in the degradation of HDPE in both *Tenebrio* species larvae, and during the biodegradation of PE as the sole carbon/energy source. Nitrogen fixation functions were stimulated in the larval gut. The larvae maintained their activities by balancing carbon and nitrogen metabolism, utilizing carbohydrates, fats or proteins selectively depending on diet type and PE PCPs. Ingestion of a PE diet promoted the enrichment of microbial motility, metabolism, and signal transduction-related pathways (e.g. two-component systems, bacterial chemotaxis, carbon metabolism, nitrogen metabolism, and PTS), which are associated with enrichments in energy, material transfer and signal transduction pathways (e.g. amino acid biosynthesis, translocator proteins and PTS).

Furthermore, the stress responses induced by LDPE, HDPE and LLDPE biodegradation processes in *Tenebrio* larvae, demonstrate that residual MP particles caused oxidative stress and negative physiological responses. Importantly, due to the high plastic degradation capabilities of *Tenebrio*, the vast majority of plastic degradation products do not pose a serious threat to the health of vertebrates or invertebrates. These findings provide novel insights into our understanding of the role of the gut microbiome in plastic-degrading insects, microplastic-induced stress responses, tissue damage and toxic effects in invertebrates and vertebrates due to MP exposure and improve our understanding of the toxicity of MPs and NPs. There are similarities, but not identical ties, between the oxidative stress induced by PE microplastics on *Tenebrio* larvae and the physiological responses of macroinvertebrates without plastic degradability. Ingestion and biodegradation of poorly degradable LLDPE or HDPE plastic polymers caused a higher degree of impairment of physiological function and metabolism in invertebrates compared to the more biodegradable LDPE plastic polymers. Follow-up studies are needed to evaluate the larval damage degree of other difficult-to-degrade or degradable plastic polymers to gain a deeper understanding of the physiological and toxicity effects associated with micro- and nanoplastics on plastic-degrading functional invertebrates, as well as to explore degradation patterns that mitigate oxidative stress in model invertebrates with plastic-degrading capabilities.

Notes

The authors declare no competing financial interest.

Availability of data and materials

This study was supported by previously published evidence of physical and chemical properties (PCPs) and polyethylene degradation by our team (Yang et al., 2022a). Meanwhile, the 16S data that support the findings of this study are available from the author upon reasonable request.

CRediT authorship contribution statement

Meng-Qi Ding: Writing – review & editing, Writing – original draft, Visualization, Validation, Methodology, Investigation, Formal analysis. **Jie Ding:** Writing – review & editing, Validation, Supervision, Funding acquisition. **Zhi-Rong Zhang:** Methodology. **Mei-Xi Li:** Methodology. **Chen-Hao Cui:** Methodology. **Ji-Wei Pang:** Methodology. **De-Feng Xing:** Methodology. **Nan-Qi Ren:** Conceptualization. **Wei-Min Wu:** Writing – review & editing, Writing – original draft, Validation, Supervision, Conceptualization. **Shan-Shan Yang:** Writing – review &

editing, Validation, Supervision, Funding acquisition.

Declaration of competing interest

The authors declare that they have no known competing financial interests or personal relationships that could have appeared to influence the work reported in this paper.

Data availability

Data will be made available on request.

Acknowledgements

The authors gratefully acknowledge the National Natural Science Foundation of China (Grant No. 52170131), the National Engineering Research Center for Bioenergy (Harbin Institute of Technology, Grant No. 2021A001) and the Open Project of State Key Laboratory of Urban Water Resource and Environment (Harbin Institute of Technology, Grant No. 2021TS03). The authors thank Professor Craig S. Criddle, Stanford University, for his support and suggestion during this study. We gratefully thank the contribution of the algorithm model and tool support by the artificial intelligence department of CECEP Digital Technology Co., Ltd. We gratefully acknowledge the support of the Heilongjiang Province Touyan Team.

Abbreviation

PCPs	physical and chemical properties
ANOVA	An analysis of variance
AWCR	average weight change rate
CR	cannibal rate
HDPE	MPs high-density polyethylene
LDPE	low-density polyethylene
LLDPE	MPs liner low-density polyethylene
MPs	microplastics
NPs	nanoplastics
Mw	weight average molecular weight
Mn	number average molecular weight
Mz	size average molecular weight
GC-MS	gas chromatography mass spectrometry
Py GC-MS	pyrolysis gas chromatography mass spectrometry
RDP	Ribosomal Database Project
OTUs	operational taxonomic units
NMDS	non-metric multidimensional scaling
db-RDA	distance-based redundancy analysis
βNTI	β-nearest taxon index
RCBray	Bray–Curtis-based Raup–Crick
PLS-SEM	Partial Least Squares- Structural equation modeling
GOF	goodness of fit
KEGG	Kyoto Encyclopedia of Genes and Genomes
KO	KEGG Orthology
VPA	variation partitioning analysis
FAPROTAX	functional Annotation of Prokaryotic Taxa
WGCNA	weighted gene co-expression network analysis
T-AOC	total antioxidant capacity
PCPs	physico-chemical properties
PE	polyethylene
SOD	superoxide dismutase
SPECR	Specific PE consumption rate
SR	survival rate
MDA	malondialdehyde
H&E	hematoxylin and eosin
LD ₅₀	the median lethal dose (50%) of the substance
LC ₅₀ (48 h)	the median lethal concentration (50%) of the substance for 48hr

QSAR	quantitative structure-activity relationship
T.E.S.T	Toxicity Estimation Software Tool

Appendix A. Supplementary data

Supplementary data to this article can be found online at <https://doi.org/10.1016/j.jenvman.2024.120832>.

References

- Al-Beloshei, N.E., Al-Awadhi, H., Al-Khalaf, R.A., Afzal, M., 2015. A comparative study of fatty acid profile and formation of biofilm in *Geobacillus gargensis* exposed to variable abiotic stress. *Can. J. Microbiol.* 61 (1), 48–59.
- Baeckhed, F., Ley, R.E., Sonnenburg, J.L., Peterson, D.A., Gordon, J.I., 2005. Host-bacterial mutualism in the human intestine. *Science* 307 (5717), 1915–1920.
- Balazs, H.E., Schmid, C.A.O., Cruzeiro, C., Podar, D., Szatmari, P.-M., Buegger, F., Hufnagel, G., Radl, V., Schroeder, P., 2021. Post-reclamation microbial diversity and functions in hexachlorocyclohexane (HCH) contaminated soil in relation to spontaneous HCH tolerant vegetation. *Sci. Total Environ.* 767.
- Bombelli, P., Howe, C.J., Bertocchini, F., 2017. Polyethylene bio-degradation by caterpillars of the wax moth *Galleria mellonella*. *Curr. Biol.* 27 (8), R292–R293.
- Brandon, A.M., Gao, S.H., Tian, R.M., Ning, D.L., Yang, S.S., Zhou, J.Z., Wu, W.M., Criddle, C.S., 2018. Biodegradation of polyethylene and plastic mixtures in mealworms (larvae of *Tenebrio molitor*) and effects on the gut microbiome. *Environ. Sci. Technol.* 52 (11), 6526–6533.
- Cappellozza, S., Leonardi, M.G., Savoldelli, S., Carminati, D., Rizzolo, A., Cortellino, G., Terova, G., Moretto, E., Badiale, A., Concheri, G., Saviane, A., Bruno, D., Bonelli, M., Caccia, S., Casartelli, M., Tettamanti, G., 2019. A first attempt to produce proteins from insects by means of a circular economy. *Animals* 9 (5).
- Chang, J.J., Tian, L., Leite, M.F.A., Sun, Y., Shi, S.H., Xu, S.Q., Wang, J.L., Chen, H.P., Chen, D.Z., Zhang, J.F., Tian, C.J., Kuramae, E.E., 2022. Nitrogen, manganese, iron, and carbon resource acquisition are potential functions of the wild rice oryza rufipogon core rhizomicrobiome. *Microbiome* 10 (1), 196–196.
- Chen, Y., Liu, X., Leng, Y., Wang, J., 2020. Defense responses in earthworms (*Eisenia fetida*) exposed to low-density polyethylene microplastics in soils. *Ecotoxicol. Environ. Saf.* 187, 109788.
- Chiellini, E., Corti, A., Swift, G., 2003. Biodegradation of thermally-oxidized, fragmented low-density polyethylenes. *Polym. Degrad. Stabil.* 81 (2), 341–351.
- Dai, T.J., Wen, D.H., Bates, C.T., Wu, L.W., Guo, X., Liu, S., Su, Y.F., Lei, J.S., Zhou, J.Z., Yang, Y.F., 2022. Nutrient supply controls the linkage between species abundance and ecological interactions in marine bacterial communities. *Nat. Commun.* 13 (1), 175.
- Ding, M.Q., Yang, S.S., Ding, J., Zhang, Z.R., Zhao, Y.L., Dai, W., Sun, H.J., Zhao, L., Xing, D., Ren, N., Wu, W.M., 2023. Gut microbiome associating with carbon and nitrogen metabolism during biodegradation of polyethylene in *Tenebrio* larvae with crop residues as Co-diets. *Environ. Sci. Technol.* 57 (8), 3031–3041.
- Dini-Andreote, F., Stegen, J.C., Elsas, V.J.D., Salles, J.F., 2015. Disentangling mechanisms that mediate the balance between stochastic and deterministic processes in microbial succession. *Proc. Natl. Acad. Sci. U.S.A.* 112 (11), E1326–E1332.
- Engel, P., Moran, N.A., 2013. The gut microbiota of insects - diversity in structure and function. *FEMS (Fed. Eur. Microbiol. Soc.) Microbiol. Rev.* 37 (5), 699–735.
- Gao, G., Wang, A., Gong, B.L., Li, Q.Q., Liu, Y.H., He, Z.M., Li, G., 2016. A novel metagenome-derived gene cluster from termite hindgut: encoding phosphotransferase system components and high glucose tolerant glucosidase. *Enzym. Microb. Technol.* 84, 24–31.
- Ghatge, S., Yang, Y., Ahn, J.-H., Hur, H.-G., 2020. Biodegradation of polyethylene: a brief review. *Applied Biological Chemistry* 63 (1).
- Glasl, B., Bourne, D.G., Fraude, P.R., Thomas, T., Schaffelke, B., Webster, N.S., 2019. Microbial indicators of environmental perturbations in coral reef ecosystems. *Microbiome* 7 (1), 94.
- Jiao, S., Yang, Y.F., Xu, Y.Q., Zhang, J., Lu, Y.H., 2020. Balance between community assembly processes mediates species coexistence in agricultural soil microbiomes across eastern China. *ISME J.* 14 (1), 202–216.
- Joop, G., Roth, O., Schmid-Hempel, P., Kurtz, J., 2014. Experimental evolution of external immune defences in the red flour beetle. *J. Evol. Biol.* 27 (8), 1562–1571.
- Kampfer, P., Ruppel, S., Remus, R., 2005. *Enterobacter radicincitans* sp nov., a plant growth promoting species of the family Enterobacteriaceae. *Syst. Appl. Microbiol.* 28 (3), 213–221.
- Kanehisa, M., Furumichi, M., Tanabe, M., Sato, Y., Morishima, K., 2017. KEGG: new perspectives on genomes, pathways, diseases and drugs. *Nucleic Acids Res.* 45 (D1), D353–D361.
- Kong, H.G., Kim, H.H., Chung, J.-H., Jun, J., Lee, S., Kim, H.-M., Jeon, S., Park, S.G., Bhak, J., Ryu, C.-M., 2019. The *Galleria mellonella* hologenome supports microbiota-independent metabolism of long-chain hydrocarbon beeswax. *Cell Rep.* 26 (9), 2451–2451.
- Kong, J., Fan, X.-D., Jia, M., 2003. Preparation of LLDPE fractions with different crystallinity via temperature rising elution fractionation. *China Plast. Ind.* 31 (9), 3 (In Chinese).
- Kundugal, H., Gangarapu, M., Sarangapani, S., Patchaiyappan, A., Devipriya, S.P., 2019. Efficient biodegradation of polyethylene (HDPE) waste by the plastic-eating lesser waxworm (*Achroia grisella*). *Environ. Sci. Pollut. Control Ser.* 26 (18), 18509–18519.

- Lambert, S., Wagner, M., 2017. Environmental performance of bio-based and biodegradable plastics: the road ahead. *Chem. Soc. Rev.* 46 (22), 6855–6871.
- Lei, L., Wu, S., Lu, S., Liu, M., Song, Y., Fu, Z., Shi, H., Raley-Susman, K.M., He, D., 2018. Microplastic particles cause intestinal damage and other adverse effects in zebrafish *Danio rerio* and nematode *Caenorhabditis elegans*. *Sci. Total Environ.* 619–620, 1–8.
- Lessa Belone, M.C., Kokko, M., Sarlin, E., 2021. Degradation of common polymers in sewage sludge purification process developed for microplastic analysis. *Environ. Pollut.* 269, 116235.
- Li, Z., Feng, C., Pang, W., Tian, C., Zhao, Y., 2021. Nanoplastics-induced genotoxicity and intestinal damage in freshwater benthic clams (*Corbicula fluminea*): comparison with microplastics. *ACS Nano.* 15 (6), 9469–9481.
- Liao, H.P., Lu, X.M., Rensing, C., Friman, V.P., Geisen, S., Chen, Z., Yu, Z., Wei, Z., Zhou, S.G., Zhu, Y.G., 2018. Hyperthermophilic composting accelerates the removal of antibiotic resistance genes and mobile genetic elements in sewage sludge. *Environ. Sci. Technol.* 52 (1), 266–276.
- Lou, Y., Ekaterina, P., Yang, S.S., Lu, B.Y., Liu, B.F., Ren, N.Q., Corvini, P.F.-X., Xing, D.F., 2020. Biodegradation of polyethylene and polystyrene by greater wax moth larvae (*Galleria mellonella* L.) and the effect of Co-diet supplementation on the core gut microbiome. *Environ. Sci. Technol.* 54 (5), 2821–2831.
- Lou, Y., Li, Y.R., Lu, B.Y., Liu, Q., Yang, S.S., Liu, B.F., Ren, N.Q., Wu, W.M., Xing, D.F., 2021. Response of the yellow mealworm (*Tenebrio molitor*) gut microbiome to diet shifts during polystyrene and polyethylene biodegradation. *J. Hazard Mater.* 416.
- Luo, L.P., Wang, Y.M., Guo, H.Q., Yang, Y.H., Qi, N., Zhao, X., Gao, S.H., Zhou, A.F., 2021. Biodegradation of foam plastics by *Zophobas atratus* larvae (Coleoptera: Tenebrionidae) associated with changes of gut digestive enzymes activities and microbiome. *Chemosphere* 282.
- Magalhaes, J.G., Tattoli, I., Girardin, S.E., 2007. The intestinal epithelial barrier: how to distinguish between the microbial flora and pathogens. *Semin. Immunol.* 19 (2), 106–115.
- Martinez-Rodriguez, J.D.C., De la Mora-Amutio, M., Plascencia-Correa, L.A., Audel-Regalado, E., Guardado, F.R., Hernandez-Sanchez, E., Pena-Ramirez, Y.J., Escalante, A., Beltran-Garcia, M.J., Ogura, T., 2014. Cultivable endophytic bacteria from leaf bases of *Agave Tequilana* and their role as plant growth promoters. *Braz. J. Microbiol.* 45 (4), 1333–1339.
- Mavriou, Z., Alexandropoulou, L., Melidis, P., Karpouzas, D.G., Ntougias, S., 2021. Biotreatment and bacterial succession in an upflow immobilized cell bioreactor fed with fludioxonil wastewater. *Environ. Sci. Pollut. Control Ser.* 28 (4), 3774–3786.
- Nicol, M., Alexandre, S., Luizet, J.-B., Skogman, M., Jouenne, T., Salcedo, S.P., De, E., 2018. Unsaturated fatty acids affect quorum sensing communication system and inhibit motility and biofilm formation of acinetobacter baumannii. *Int. J. Mol. Sci.* 19 (1).
- Núria, S.-B., Ribas, L., Piferrer, F., 2022. Improved biomarker discovery through a plot twist in transcriptomic data analysis. *BMC Biol.* 20 (1).
- Nyholm, S.V., Graf, J., 2012. Knowing your friends: invertebrate innate immunity fosters beneficial bacterial symbioses. *Nat. Rev. Microbiol.* 10 (12), 815–827.
- Ojeda, T., Freitas, A., Birck, K., Dalmolin, E., Jacques, R., Bento, F., Camargo, F., 2011a. Degradability of linear polyolefins under natural weathering. *Polym. Degrad. Stabil.* 96 (4), 703–707.
- Ojeda, T., Freitas, A., Birck, K., Dalmolin, E., Jacques, R., Bento, F., Camargo, F., 2011b. Degradability of linear polyolefins under natural weathering. *Polym. Degrad. Stabil.* 96 (4), 703–707.
- Palmer, J.D., Foster, K.R., 2022. Bacterial species rarely work together. *Science* 376 (6593), 581–582.
- Peng, B.-Y., Sun, Y., Wu, Z., Chen, J., Shen, Z., Zhou, X., Wu, W.-M., Zhang, Y., 2022. Biodegradation of polystyrene and low-density polyethylene by *Zophobas atratus* larvae: fragmentation into microplastics, gut microbiota shift, and microbial functional enzymes. *J. Clean. Prod.* 367.
- Peng, B.-Y., Xu, Y., Sun, Y., Xiao, S., Sun, J., Shen, Z., Chen, J., Zhou, X., Zhang, Y., 2023a. Biodegradation of polyethylene (PE) microplastics by mealworm larvae: physiological responses, oxidative stress, and residual plastic particles. *J. Clean. Prod.* 402.
- Peng, B.Y., Chen, Z., Chen, J., Yu, H., Zhou, X., Criddle, C.S., Wu, W.M., Zhang, Y., 2020. Biodegradation of polyvinyl chloride (PVC) in *Tenebrio molitor* (Coleoptera: Tenebrionidae) larvae. *Environ. Int.* 145, 106106.
- Peng, B.Y., Chen, Z.B., Chen, J.B., Zhou, X.F., Wu, W.M., Zhang, Y.L., 2021. Biodegradation of polylactic acid by yellow mealworms (larvae of *Tenebrio molitor*) via resource recovery: a sustainable approach for waste management. *J. Hazard Mater.* 416, 125803.
- Peng, B.Y., Su, Y., Chen, Z., Chen, J., Zhou, X., Benbow, M.E., Criddle, C.S., Wu, W.-M., Zhang, Y., 2019. Biodegradation of polystyrene by dark (*Tenebrio obscurus*) and yellow (*Tenebrio molitor*) mealworms (Coleoptera: Tenebrionidae). *Environ. Sci. Technol.* 53 (9), 5256–5265.
- Peng, B.Y., Sun, Y., Zhang, X., Sun, J., Xu, Y., Xiao, S., Chen, J., Zhou, X., Zhang, Y., 2023b. Unveiling the residual plastics and produced toxicity during biodegradation of polyethylene (PE), polystyrene (PS), and polyvinyl chloride (PVC) microplastics by mealworms (Larvae of *Tenebrio molitor*). *J. Hazard Mater.* 452, 131326.
- PlasticsEurope, 2024. Plastics – the Fast Facts 2023.
- Prata, J.C., da Costa, J.P., Girão, A.V., Lopes, I., Duarte, A.C., Rocha-Santos, T., 2019. Identifying a quick and efficient method of removing organic matter without damaging microplastic samples. *Sci. Total Environ.* 686, 131–139.
- Przemieniecki, S.W., Kosewska, A., Ciesielski, S., Kosewska, O., 2020. Changes in the gut microbiome and enzymatic profile of *Tenebrio molitor* larvae biodegrading cellulose, polyethylene and polystyrene waste. *Environ. Pollut.* 256 (2020), 113265.
- Qin, Y., Song, F., Ai, Z., Zhang, P., Zhang, L., 2015. Protocatechuic acid promoted alachlor degradation in Fe(III)/H₂O₂ Fenton system. *Environ. Sci. Technol.* 49 (13), 7948–7956.
- Ren, Y., Yu, G., Shi, C.P., Liu, L.M., Guo, Q., Han, C., Zhang, D., Zhang, L., Liu, B.X., Gao, H., Zeng, J., Zhou, Y., Qiu, Y.H., Wei, J., Luo, Y.C., Zhu, F.J., Li, X.J., Wu, Q., Li, B., Fu, W.Y., Tong, Y.L., Meng, J., Fang, Y.H., Dong, J., Feng, Y.T., Xie, S.C., Yang, Q.Q., Yang, H., Wang, Y., Zhang, J.B., Gu, H.D., Xuan, H.D., Zou, G.Q., Luo, C., Huang, L., Yang, B., Dong, Y.C., Zhao, J.H., Han, J.C., Zhang, X.L., Huang, H.S., 2022. Majorbio Cloud: a one-stop, comprehensive bioinformatic Platform for multiomics analyses. *iMeta* 1 (2).
- Restrepo-Florez, J.-M., Bassi, A., Thompson, M.R., 2014. Microbial degradation and deterioration of polyethylene - a review. *Int. Biodeterior. Biodegrad.* 88, 83–90.
- Robinson, W.H., 2005. Urban Insects and Arachnids: a Handbook of Urban Entomology. Cambridge University Press.
- Ru, J., Huo, Y., Yang, Y., 2020. Microbial degradation and valorization of plastic wastes. *Front. Microbiol.* 11, 442.
- Ruiz Barriosueño, J.M., Martin, E., Galindo Cardona, A., Malizia, A., Chalup, A., de Cristobal, R.E., Monmany Garzia, A.C., 2022a. Consumption of low-density polyethylene, polypropylene, and polystyrene materials by larvae of the greater wax moth, *Galleria mellonella* L. (Lepidoptera, Pyralidae), impacts on their ontogeny. *Environ. Sci. Pollut. Res. Int.* 29 (45), 68132–68142.
- Ruiz Barriosueño, J.M., Vilanova-Cuevas, B., Alvarez, A., Martin, E., Malizia, A., Galindo-Cardona, A., de Cristobal, R.E., Occhionero, M.A., Chalup, A., Monmany-Garzia, A.C., Godoy-Vitorino, F., 2022b. The bacterial and fungal gut microbiota of the greater wax moth, *Galleria mellonella* L. Consuming polyethylene and polystyrene. *Front. Microbiol.* 13, 918861.
- Sahu, U., Theertha, D.P., Maslad, N., Madhurya, L., Vendan, S.E., 2023. Physico-chemical stress alters cuticular semiochemical secretions in the red flour beetle, *Tribolium castaneum* adults. *J. Pest. Sci.* <https://doi.org/10.1007/s10340-023-01692-8>.
- Sanchez-Hernandez, J.C., 2021. A toxicological perspective of plastic biodegradation by insect larvae. *Comparative Biochemistry and Physiology C-Toxicology & Pharmacology* 248.
- Scopetani, C., Chelazzi, D., Mikola, J., Leinio, V., Heikkinen, R., Cincinelli, A., Pellinen, J., 2020. Olive oil-based method for the extraction, quantification and identification of microplastics in soil and compost samples. *Sci. Total Environ.* 733, 139338.
- Shah, A.A., Hasan, F., Akhter, J.I., Hameed, A., Ahmed, S., 2008. Degradation of polyurethane by novel bacterial consortium isolated from soil. *Ann. Microbiol.* 58 (3), 381–386.
- Shi, C., Han, X., Guo, W., Wu, Q., Yang, X., Wang, Y., Tang, G., Wang, S., Wang, Z., Liu, Y., Li, M., Lv, M., Guo, Y., Li, Z., Li, J., Shi, J., Qu, G., Jiang, G., 2022. Disturbed Gut-Liver axis indicating oral exposure to polystyrene microplastic potentially increases the risk of insulin resistance. *Environ. Int.* 164.
- Stegen, J.C., Lin, X.J., Fredrickson, J.K., Chen, X.Y., Kennedy, D.W., Murray, C.J., Rockhold, M.L., Konopka, A., 2013. Quantifying community assembly processes and identifying features that impose them. *ISME J.* 7 (11), 2069–2079.
- Suppiger, A., Aguilar, C., Eberl, L., 2016. Evidence for the widespread production of DSF family signal molecules by members of the genus *Burkholderia* by the aid of novel biosensors. *Environmental Microbiology Reports* 8 (1), 38–44.
- Suzuki, K., Meek, B., Doi, Y., Muramatsu, M., Chiba, T., Honjo, T., Fagarasan, S., 2004. Aberrant expansion of segmented filamentous bacteria in IgA-deficient gut. *Proc. Natl. Acad. Sci. U.S.A.* 7, 101.
- Tripathi, B.M., Stegen, J.C., Kim, M., Dong, K., Adams, J.M., Lee, Y.K., 2018. Soil pH mediates the balance between stochastic and deterministic assembly of bacteria. *ISME J.* 12 (4), 1072–1083.
- van Broekhoven, S., Oonincx, D.G., van Loon, J.J., 2015. Growth performance and feed conversion efficiency of three edible mealworm species (Coleoptera: Tenebrionidae) on diets composed of organic by-products. *J. Insect Physiol.* 73, 1–10.
- Wagg, C., Bender, S.F., Widmer, F., van der Heijden, M.G.A., 2014. Soil biodiversity and soil community composition determine ecosystem multifunctionality. *Proc. Natl. Acad. Sci. U.S.A.* 111 (14), 5266–5270.
- Welti, E.A.R., Roeder, K.A., de Beurs, K.M., Joern, A., Kaspari, M., 2020. Nutrient dilution and climate cycles underlie declines in a dominant insect herbivore. *Proc. Natl. Acad. Sci. U.S.A.* 117 (13), 7271–7275.
- Wilkes, R.A., Aristilde, L., 2017. Degradation and metabolism of synthetic plastics and associated products by *Pseudomonas* sp.: capabilities and challenges. *J. Appl. Microbiol.* 123 (3), 582–593.
- Woo, S., Song, I., Cha, H.J., 2020. Fast and facile biodegradation of polystyrene by the gut microbial flora of *plesiophthalmus davidi*s larvae. *Appl. Environ. Microbiol.* 86 (18).
- Wu, R., Sun, J.Y., Zhao, L.L., Fan, Z.N., Yang, C., 2020. Systematic identification of key functional modules and genes in gastric cancer. *BioMed Res. Int.* 2020, 1–16.
- Wu, R., Zhuang, H., Mei, Y.K., Sun, J.Y., Dong, T., Zhao, L.L., Fan, Z.N., Liu, L., 2021. Systematic identification of key functional modules and genes in esophageal cancer. *Cancer Cell Int.* 21 (1), 134.
- Wu, W.M., Criddle, C.S., 2021. Characterization of biodegradation of plastics in insect larvae. *Methods Enzymol.* 648, 95–120.
- Xue, C., Li, L., Guo, C., Gao, Y., Yang, C., Deng, X., Li, X., Tai, P., Sun, L., 2023. Understanding the role of graphene oxide in affecting PAHs biodegradation by microorganisms: an integrated analysis using 16S rRNA, metatranscriptomic, and metabolomic approaches. *J. Hazard Mater.* 457, 131811.
- Xue, L., Ren, H.D., Brodrrib, T.J., Wang, J., Yao, X.H., Li, S., 2020. Long term effects of management practice intensification on soil microbial community structure and Co-occurrence network in a non-timber plantation. *For. Ecol. Manag.* 459.
- Yang, Y., Hu, L., Li, X., Wang, J.L., Jin, G.S., 2023a. Nitrogen Fixation and Diazotrophic Community in Plastic-Eating Mealworms *Tenebrio molitor* L. *Microb. Ecol.* 85, 264–276.

- Yang, J., Yang, Y., Wu, W.-M., Zhao, J., Jiang, L., 2014. Evidence of polyethylene biodegradation by bacterial strains from the guts of plastic-eating waxworms. Environ. Sci. Technol. 48 (23), 13776–13784.
- Yang, L., Gao, J., Liu, Y., Zhuang, G.Q., Peng, X.W., Wu, W.M., Zhuang, X.L., 2021a. Biodegradation of expanded polystyrene and low-density polyethylene foams in larvae of *Tenebrio molitor* linnaeus (Coleoptera: Tenebrionidae): broad versus limited extent depolymerization and microbe-dependence versus independence. Chemosphere 262, 127818.
- Yang, S.S., Ding, M.Q., He, L., Zhang, C.H., Li, Q.X., Xing, D.F., Cao, G.L., Zhao, L., Ding, J., Ren, N.Q., Wu, W.M., 2021b. Biodegradation of polypropylene by yellow mealworms (*Tenebrio molitor*) and superworms (*Zophobas atratus*) via gut-microbe-dependent depolymerization. Sci. Total Environ. 756, 144087.
- Yang, S.S., Ding, M.Q., Ren, X.R., Zhang, Z.R., Li, M.X., Zhang, L.L., Pang, J.W., Chen, C.X., Zhao, L., Xing, D.F., Ren, N.Q., Ding, J., Wu, W.M., 2022. Impacts of physical-chemical property of polyethylene on depolymerization and biodegradation in yellow and dark mealworms with high purity microplastics. Sci. Total Environ. 828, 154458.
- Yang, S.S., Ding, M.Q., Zhang, Z.R., Ding, J., Bai, S.W., Cao, G.L., Zhao, L., Pang, J.W., Xing, D.F., Ren, N.Q., Wu, W.M., 2021c. Confirmation of biodegradation of low-density polyethylene in dark- versus yellow- mealworms (larvae of *Tenebrio obscurus* versus *Tenebrio molitor*) via Gut microbe-independent depolymerization. Sci. Total Environ. 789, 147915.
- Yang, Y., Yang, J., Wu, W.-M., Zhao, J., Song, Y.L., Gao, L.C., Yang, R.F., Jiang, L., 2015a. Biodegradation and mineralization of polystyrene by plastic-eating mealworms: Part 1. Chemical and physical characterization and isotopic tests. Environ. Sci. Technol. 49 (20), 12080–12086.
- Yang, Y., Yang, J., Wu, W.M., Zhao, J., Song, Y.L., Gao, L.C., Yang, R.F., Jiang, L., 2015b. Biodegradation and mineralization of polystyrene by plastic-eating mealworms: Part 2. Role of gut microorganisms. Environ. Sci. Technol. 49 (20), 12087–12093.
- Yezerski, A., Gilnor, T.P., Stevens, L., 2004. Genetic analysis of benzoquinone production in *Tribolium confusum*. J. Chem. Ecol. 30 (5), 1035–1044.
- Zhang, F., Wang, Z., Vijver, M.G., Peijnenburg, W., 2022a. Theoretical investigation on the interactions of microplastics with a SARS-CoV-2 RNA fragment and their potential impacts on viral transport and exposure. Sci. Total Environ. 842, 156812.
- Zhang, Y.H., Zhao, Y.Y., 2019. The complete mitochondrial genome of dark mealworm *Tenebrio obscurus* (Coleoptera: Tenebrionidae). Mitochondrial DNA B Resour 4 (2), 2560–2561.
- Yu, J.C., Sundqvist, B., Tonpheng, B., Andersson, O., 2014. Thermal conductivity of highly crystallized polyethylene. Polymer 55 (1), 195–200.
- Zhang, Z., Peng, H.R., Yang, D.C., Zhang, G.Q., Zhang, J.L., Ju, F., 2022b. Polyvinyl chloride degradation by a bacterium isolated from the gut of insect larvae. Nat. Commun. 13 (1).
- Zhou, L., Liu, L., Chen, W.Y., Sun, J.J., Hou, S.W., Kuang, T.X., Wang, W.X., Huang, X.D., 2020. Stochastic determination of the spatial variation of potentially pathogenic bacteria communities in a large subtropical river. Environ. Pollut. 264, 114683.
- Zielinska, E., Zielinski, D., Jakubczyk, A., Kara, M., Lewicki, S., 2021. The impact of polystyrene consumption by edible insects *Tenebrio molitor* and *Zophobas morio* on their nutritional value, cytotoxicity, and oxidative stress parameters. Food Chem. 345 (1), 128846.
- Yang, S.S., Wu, W.M., Pang, J.W., He, L., Ding, M.Q., Li, M.X., Zhao, Y.L., Sun, H.J., Xing, D.F., Ren, N.Q., Yang, J., Criddle, C.S., Ding, J., 2023b. Bibliometric analysis of publications on biodegradation of plastics: Explosively emerging research over 70 years. J. Clean. Prod. 428.